frontiers in
MICROBIOLOGY

ORIGINAL RESEARCH ARTICLE
published: 10 February 2011
doi: 10.3389/fmicb.2011.00017

Sulfur metabolism in the extreme acidophile *Acidithiobacillus caldus*

Stefanie Mangold[1]*, Jorge Valdés[2,3†], David S. Holmes[2,3] and Mark Dopson[1†]

[1] *Department of Molecular Biology, Umeå University, Umeå, Sweden*
[2] *Center for Bioinformatics and Genome Biology, Fundación Ciencia para Vida, Santiago, Chile*
[3] *Departamento de Ciencias Biologicas, Andrés Bello University, Santiago, Chile*

Edited by:
Thomas E. Hanson, University of Delaware, USA

Reviewed by:
Kathleen Scott, University of South Florida, USA
Dimitry Y. Sorokin, Delft University of Technology, Netherlands

****Correspondence:***
Stefanie Mangold, Department of Molecular Biology, Umeå University, SE-901 87 Umeå, Sweden.
e-mail: stefanie.mangold@miolbiol.umu.se

†Current address:
Jorge Valdés, Bio-Computing Laboratory, Fraunhofer-Chile Research Foundation, Santiago, Chile;
Mark Dopson, Institution for Natural Sciences, Linnaeus University, 391 82 Kalmar, Sweden.

Given the challenges to life at low pH, an analysis of inorganic sulfur compound (ISC) oxidation was initiated in the chemolithoautotrophic extremophile *Acidithiobacillus caldus*. *A. caldus* is able to metabolize elemental sulfur and a broad range of ISCs. It has been implicated in the production of environmentally damaging acidic solutions as well as participating in industrial bioleaching operations where it forms part of microbial consortia used for the recovery of metal ions. Based upon the recently published *A. caldus* type strain genome sequence, a bioinformatic reconstruction of elemental sulfur and ISC metabolism predicted genes included: sulfide–quinone reductase (*sqr*), tetrathionate hydrolase (*tth*), two *sox* gene clusters potentially involved in thiosulfate oxidation (*soxABXYZ*), sulfur oxygenase reductase (*sor*), and various electron transport components. RNA transcript profiles by semi quantitative reverse transcription PCR suggested up-regulation of *sox* genes in the presence of tetrathionate. Extensive gel based proteomic comparisons of total soluble and membrane enriched protein fractions during growth on elemental sulfur and tetrathionate identified differential protein levels from the two Sox clusters as well as several chaperone and stress proteins up-regulated in the presence of elemental sulfur. Proteomics results also suggested the involvement of heterodisulfide reductase (HdrABC) in *A. caldus* ISC metabolism. A putative new function of Hdr in acidophiles is discussed. Additional proteomic analysis evaluated protein expression differences between cells grown attached to solid, elemental sulfur versus planktonic cells. This study has provided insights into sulfur metabolism of this acidophilic chemolithotroph and gene expression during attachment to solid elemental sulfur.

Keywords: *Acidithiobacillus caldus*, elemental sulfur, inorganic sulfur compounds, metabolism, attachment, proteomics

INTRODUCTION

Inorganic sulfur compounds (ISCs) in acidic, sulfide mineral environments are produced as a result of abiotic Fe(III) oxidation of sulfide minerals such as pyrite (FeS_2; initial ISC product is thiosulfate) or chalcopyrite ($CuFeS_2$; initial product is polysulfide sulfur). Their subsequent biooxidation produces sulfuric acid as the final product (Schippers and Sand, 1999; Johnson and Hallberg, 2009). As a result of sulfuric acid production, sulfide mineral environments are typically inhabited by acidophilic microorganisms. These microorganisms are exploited in the biotechnological process of "Biomining" whereby dissolution of sulfide minerals is catalyzed by the action of ISC oxidizing microorganisms as well as Fe(II) oxidizers that regenerate the Fe(III) required for the abiotic attack of sulfide minerals (Rawlings and Johnson, 2007).

A diverse range of acidophilic or neutrophilic photo- and chemolithotrophs can oxidize ISCs from sulfide (oxidation state of −2) to sulfate (+6; reviewed in Ghosh and Dam, 2009). Microorganisms utilize several systems for ISC oxidation including the *Paracoccus pantotrophus* 15 gene sulfur oxidizing (*sox*) cluster. This cluster encodes the multiple substrate Sox system that catalyzes oxidation of thiosulfate, elemental sulfur (S^0), sulfide, and sulfite to sulfate. SoxAX is composed of the dihemic and monohemic cytochromes SoxA and SoxX, respectively. SoxYZ is predicted to be able to bind ISCs in different oxidation states by the cysteine contained in the V-K-V-T-I-G-G-C-G-G conserved motif on the carboxy terminus of the protein. The SoxB subunit is predicted to have two manganese ions in the active site and works as a sulfate thiohydrolase interacting with SoxYZ (Friedrich et al., 2005). Several sulfur oxidizing bacteria (e.g., green and purple sulfur bacteria) only contain the core thiosulfate oxidizing multi-enzyme system (TOMES). The TOMES lacks the sulfur dehydrogenase $Sox(CD)_2$ and oxidizes thiosulfate to sulfate and S^0 (reviewed in Friedrich et al., 2001; Ghosh and Dam, 2009, and Sakurai et al., 2010). Due to the lack of $Sox(CD)_2$, S^0 is polymerized to form globules which can be further oxidized by proteins encoded in the dissimilatory sulfite reductase (*dsr*) gene cluster (Hensen et al., 2006).

In contrast to the well studied Sox enzyme complex, the ISC oxidations pathways in acidophiles are not very well understood. As described in recent reviews (Rohwerder and Sand, 2007; Johnson and Hallberg, 2009), S^0 is thought to be oxidized by acidophilic bacteria via sulfur dioxygenase (SDO) and by archaea via sulfur oxygenase reductase (Sor). The SDO has not been characterized although its enzyme activity has been shown (Suzuki, 1999; Rohwerder and Sand, 2003). However, the archaeal Sor has been well studied and the corresponding gene has been identified in *Acidianus tengchongensis*, *Aquifex aeolicus*, *Picrophilus torridus*, "*Ferroplasma acidarmanus*," and *Sulfolobus tokodaii* (Urich et al.,

2006). In the presence of oxygen, Sor simultaneously catalyzes oxidation and reduction of S^0 generating sulfite, thiosulfate, and sulfide (Urich et al., 2006). The enzyme does not require cofactors or external electron donors for S^0 reduction. Due to its cytoplasmic location it is believed that it does not play a role in formation of the transmembrane electron gradient but rather provide substrates for other membrane bound enzymes. Another enzyme which has recently been suggested to be involved in *Acidithiobacillus ferrooxidans* S^0 metabolism is heterodisulfide reductase (Hdr; Quatrini et al., 2009). So far no biochemical evidence for *A. ferrooxidans* S^0 oxidation by Hdr has been reported, however, transcriptomics (Quatrini et al., 2009) and proteomics data (unpublished data) strongly suggests its involvement. Hdr of methanogenic archaea has been studied (Hedderich et al., 2005) and it catalyzes the reversible reduction of the disulfide bond in heterodisulfide accompanied by the extrusion of electrons and the formation of a transmembrane electron gradient. Quatrini et al. (2009) hypothesize that Hdr works in reverse in acidophiles by utilizing the naturally existing proton gradient to oxidize disulfide intermediates originating from S^0 and donating electrons to the quinone pool. Other enzymes involved in acidophilic ISC oxidation pathways are thiosulfate:quinone oxidoreductase (Tqr) which oxidizes thiosulfate to tetrathionate, tetrathionate hydrolase (Tth), and sulfide oxidoreductase (Rohwerder and Sand, 2007; Johnson and Hallberg, 2009). Recently, the analysis of gene context has highlighted differences in ISC oxidation strategies in *A. ferrooxidans*, *Acidithiobacillus thiooxidans*, and *Acidithiobacillus caldus* (Cardenas et al., 2010). Microarray analysis suggests the *petII* (prosthetic group-containing subunits of the cytochrome bc_1 complex), *cyo* (cytochrome *o* ubiquinol oxidase), *cyd* (cytochrome *bd* ubiquinol oxidase), and *doxII* (encoding thiosulfate quinol reductase) gene clusters are up-regulated during growth on S^0 compared to Fe(II) grown cells (Quatrini et al., 2006). From these data, a model for *A. ferrooxidans* ISC metabolism has been created (Quatrini et al., 2009). *A. ferrooxidans* proteins with increased expression during growth on S^0 include an outer membrane protein (Omp40) and a thiosulfate sulfur transferase protein (Ramirez et al., 2004). Also, a high throughput study of periplasmic proteins identified 41 and 14 proteins uniquely expressed in S^0 and thiosulfate grown cells, respectively (Valenzuela et al., 2008). The genome context of these proteins suggests they are involved in ISC metabolism and possibly S^0 oxidation and Fe–S cluster construction. Secreted proteins from a pure culture of *A. thiooxidans* and from co-culture with *A. ferrooxidans* were studied by proteomics (Bodadilla Fazzini and Parada, 2009). An Omp40 like protein was identified which is suggested to be involved in attachment. Finally, S^0 induced genes in the acidophilic archaeon *Sulfolobus metallicus* include Sor (Bathe and Norris, 2007).

A. caldus is an ISC oxidizing acidophile (Hallberg et al., 1996b) often identified in biomining environments (Okibe et al., 2003; Dopson and Lindström, 2004). *A. caldus* aids in metal dissolution by removal of solid S^0 that may form a passivating layer on the mineral surface (Dopson and Lindström, 1999). The *A. caldus* draft genome contains genes for ISC oxidation (Valdes et al., 2009). The gene cluster containing the *A. caldus* tetrathionate hydrolase (*tth*) and the *doxD* component (thiosulfate:quinol oxidoreductase) has been characterized (Rzhepishevska et al., 2007). The Tth is a periplasmic homo-dimer with an optimum pH of 3 (Bugaytsova and Lindström, 2004). Previously Tth was also studied in *A. ferrooxidans* (de Jong et al., 1997).

Owing to the fact that *A. caldus* is ubiquitous in both natural and anthropogenic sulfide mineral environments, its importance in generating sulfuric acid, and in mitigating mineral passivation we have investigated its ISC metabolism. An in depth bioinformatic analysis revealed the putative genes responsible for sulfuric acid generation, that have then been verified by proteomic comparison between growth with tetrathionate and S^0 and via transcript profiling. This has generated insights into the ISC metabolism of this microorganism. Such knowledge might help to better understand the industrial processes.

MATERIALS AND METHODS

BIOINFORMATIC RECONSTRUCTION OF *A. CALDUS* ISC METABOLISM

Genes and metabolic pathways involved in ISC and S^0 oxidation/reduction were obtained from Metacyc[1] and Kegg[2]. Amino acid sequences derived from selected genes previously identified to be involved in ISC metabolism were used as a query to conduct BlastP and tBlastN (Altschul et al., 1997) searches to interrogate the *A. caldus*^{T} (ATCC51756) draft genome sequence (NZ_ACVD00000000.1). Potential gene candidates were further characterized employing the following bioinformatic tools: ClustalW (Larkin et al., 2007) for primary structure similarity relations, PSI-PRED (Bryson et al., 2005) for secondary structure predictions, Prosite (Hulo et al., 2006) for motif predictions, and ProDom (Bru et al., 2005) and Pfam (Finn et al., 2008) for domain predictions. Selected gene candidates were assigned to putative orthologous groups in order to determine potential evolutionary associations[3] (Tatusov et al., 2003). Information regarding the organization of genes in other S^0 metabolizing microorganisms was obtained from NCBI[4] and IMG–JGI[5].

MEDIA AND CULTURE CONDITIONS

A. caldus^T was cultured in mineral salts medium (MSM) with trace elements (Dopson and Lindström, 1999) at 45°C and pH 2.5 whilst sparging with 2% (vol/vol) CO_2 enriched air. Tetrathionate (5 mM; Sigma) and 5 g/L hydrophilic, biologically produced S^0 (provided by PAQUES B.V., the Netherlands) were used as substrate. Stock solutions of tetrathionate were sterile filtered and added to the autoclaved (121°C for 15 min) MSM, whereas the finely ground S^0 was added to MSM prior to autoclaving at 105°C for 30 min. The medium containing solid S^0 was stirred for 24 h to ensure fine dispersion of the S^0 particles. Biomass for the transcript profiling and proteomic comparison of growth on tetrathionate versus S^0 was produced in continuous culture with a dilution rate of 0.06 h^{-1}. The homogeneous delivery of solid substrate was ensured by continuous stirring of the feed vessel and an appropriate flow rate which did not allow S^0 to settle in the tubing. In contrast, cell mass for proteomic comparison of *A. caldus* sessile versus planktonic

[1]http://metacyc.org/

[2]http://www.genome.ad.jp/kegg/

[3]http://www.ncbi.nlm.nih.gov/COG/

[4]http://www.ncbi.nlm.nih.gov/genome/

[5]http://genome.jgi-psf.org/programs/bacteria-archaea/index.jsf

growth was grown in 1 L batch cultures with initial pH 2.5. Sessile and planktonic bacteria from batch cultures were harvested in mid exponential growth phase according to planktonic cell counts (pH at collection was 1.3–1.4). Planktonic cells from batch or continuous culture were harvested at 4750 g for 10 min followed by a washing step in MSM pH 2.5. For the continuous culture grown on S^0, the remaining S^0 particles were separated from planktonic cells by pelleting at 450 g for 30 s which only removed the S^0 but left planktonic cells in the supernatant (the solid S^0 and any attached cells were discarded). Solid S^0 with sessile bacteria attached was collected from batch cultures and washed four times with MSM pH 2.5 until no planktonic bacteria were detected in the supernatant by microscopic investigation before pelleting at 450 g for 30 s. All cell and S^0 pellets were stored at −80°C.

SEMI QUANTITATIVE RNA TRANSCRIPT PROFILES

Primers targeting selected genes putatively involved in ISC metabolism were designed for semi quantitative reverse transcription (RT-) PCR amplification (product sizes 98–530 bp; **Table 1**). RNA was extracted from 100 to 200 mL medium from the continuous cultures with TRI reagent (Ambion) according to the manufacturer's recommendations. Contaminating DNA was digested with RNase-free DNase I (Fermentas) followed by a second extraction with TRI reagent. RNA concentration and purity was measured with a NanoDrop 2000 spectrophotometer (ThermoScientific). In order to rule out DNA contamination, the RNA samples were subjected to PCR using illustra PuRE Taq Ready-To-Go PCR Beads (GE Healthcare). RT-PCR was performed in a two step reaction using RevertAid First Strand cDNA Synthesis Kit (Fermentas) for RT and AccessQuick Master Mix (Promega) for PCR. The RT reaction primed with random hexamers was performed with 1 µg total RNA for 1 h at 45°C using two independent biological samples for each condition. PCR primed with specific primers (**Table 1**) was carried out with 1 µL of RT reaction as template in 25 µL reaction volume in PTC-100 Programmable Thermal Controller (MJ Research Inc.). PCR cycling was started with initial denaturation at 95°C for 5 min, followed by 30 amplification cycles consisting of denaturation at 95°C for 30 s, annealing at primer specific temperatures (**Table 1**) for 30 s, and elongation at 72°C for 2 min 30 s and concluded with 5 min elongation at 72°C (no further increase of PCR product was observed after 31 cycles). A transcription control gene, DNA gyrase (*gyrA*), was used (Takle et al., 2007). PCR products were separated by agarose electrophoresis and quantified with QuantityOne (BioRad). For final analysis, the 2 independent RNA samples (biological replicates) were used as templates for duplicate RT-PCR reactions (technical replicates) which yielded a total of four replications. In a few cases one replicate was not considered for analysis.

Table 1 | Primers used for RNA transcript profiles.

Primer name	Primer sequence	Targeted gene	Product size [bp]	Melting temp. [°C]
ACA0302For	TTCGAGCAACTCCTGCAGACG	*sor*	271	55.5
ACA0302Rev	CGTCCGTCATACCCATGATCC	ACA_0302		
ACA1632For	GATCCAGGCGATTCATATACGG	*doxD*	337	55.5
ACA1632Rev	TGATCCCCATAGCGAAATTAGAG	ACA_1632		
ACA1633For	TTTTGCGCGTTTGTACCTACCC	*tth*	223	55.5
ACA1633Rev	AACGCCGTCTACTTGAGCTCC	ACA_1633		
ACA2312For	TGGCGATCTTACCTTGAGCGAGG	*soxA*-I	436	55.5
ACA2312Rev	TGCGCTCTGCCCCAAAAGTGG	ACA_2312		
ACA2392For	ATCTACCCTTCGACAAGTATGC	*soxA*-II	527	55.5
ACA2392Rev	TGTGCCGTCTCGCCTTGCAAG	ACA_2392		
ACA2317For	GAAGCCGGTACTGATCAACAAG	*soxB*-I	437	55.5
ACA2317Rev	CGTGTACTCCGTAACCGTAACC	ACA_2317		
ACA2394For	TCCGTCCTCAACCAGACGCCC	*soxB*-II	467	55.5
ACA2394Rev	ACAGCGATTTTGCGACCGCTG	ACA_2394		
ACA2319For	CTCGCGCCGCAAATGTTCCCG	*soxY*-I	180	55.5
ACA2319Rev	TGATCGACATCCACGGTAACCG	ACA_2319		
ACA2390For	ATCGGCACAAGCCTCGTTGCG	*soxY*-II	340	55.5
ACA2390Re2	CTGGGGTGAGATCGAACTGGC	ACA_2390		
ACA2313For	GTGCAGTTTATTTACGACCCGG	*soxX*-I	98	58
ACA2313Rev	ACCAAGCCAATCTGGTGATCCG	ACA_2313		
ACA2389For	ACTCGATACCATCGTTCGTGC	*soxX*-II	256	58
ACA2389Rev	TCTGGAACATCTGCTGGAAGG	ACA_2389		
ACA2318For	AGAGGTCCGTTCGTTGATCATG	*soxZ*-I	269	58
ACA2318Rev	TCAGGCGACGGTGATCTTTGCC	ACA_2318		
ACA2391For	ATGGCAGACAATATTGGTAACCC	*soxZ*-II	197	58
ACA2391Rev	TCGATGTCCAGCAGCTTTGCAC	ACA_2391		
ACAgyrA-F4	CAGCCTCGAAAAAGAAATGC	*gyrA*	431	55.5
ACAgyrA-R4	CCACCTCCTTCTCGTCGTAG	ACA_1592		

A. CALDUS PROTEOMICS ANALYSIS

For the preparation of the total soluble proteome, cell pellets from 200 mL culture were re-suspended in lysis buffer (7 M urea, 2 M thiourea, 30 mM Tris, 1 mM EDTA, 1.5% Triton X-100, pH 8.5), broken by sonication (2 min, 5 s pulse, 5 s break, 30% amplitude), cell debris removed by centrifugation (10 min, 10 000 rpm, 4°C), and the lysate stored at −80°C. Isoelectric focusing (IEF) was performed using pre-cast, 18 cm, Immobiline DryStrip IPG gels (GE Healthcare) with a non-linear pH gradient from 3 to 10 in an Ettan IPGphor IEF unit (GE Healthcare). Protein samples (200 µg) were applied to the IPG strip in rehydration buffer (7 M urea, 2 M thiourea, and 1.5% Triton X-100) with 1.45% dithiothreitol (DTT) and 0.5% IPG buffer (GE Healthcare). After passive rehydration for 16 h at 25°C, IEF was run for a total of 42 kVh with stepwise increasing voltage according to supplier's recommendation. Following IEF, the gel strips were equilibrated in two steps using equilibration buffer (75 mM Tris, 6 M urea, 30% glycerol, 2% SDS) with additional 100 mM DTT in the first step and equilibration buffer with 2.5% iodoacetamide in the second step. The gel strips were then applied to 12% Duracryl (NextGene Genomic Solutions) SDS-polyacrylamide gels and sealed with 1.5% (wt/vol) agarose solution containing bromophenol blue. Electrophoresis was run in an Ettan DALTsix apparatus (GE Healthcare). The gels were fixed and stained to saturation with colloidal Coomassie (Anderson, 1991). After staining was completed the gels were scanned using Image Scanner (GE Healthcare) and analyzed using image analysis software Melanie 7.03 (Genebio). The membrane enriched fractions were prepared according to Molloy (2008). In brief, crude cell extracts were obtained by sonication in Tris buffer (50 mM Tris pH 8.0, 0.5 mM EDTA) and enriched for bacterial membranes by incubation at 4°C for 1 h in 100 mM Na_2CO_3 and subsequent ultracentrifugation at 170 000 g for 70 min. This carbonate extraction in combination with membrane solubilization and 2D gel electrophoresis has been used for the recovery of outer membrane proteins of Gram-negative bacteria (Molloy et al., 2000, 2001; Phadke et al., 2001). The pellets were washed with 50 mM Tris buffer pH 8.0 and re-suspended overnight at 4°C in rehydration buffer. The protocol for 2D gels was the same as above except that 24 cm IPG strips were used and IEF was run for a total of 59 kVh. For the preparation of the soluble protein fraction from sessile bacteria it was necessary to detach the cells from the S^0 prior to protein extraction and 2D gel electrophoresis (as above). The method for cell detachment by Gehrke et al. (1998) was modified. In brief, the S^0 with sessile cells was incubated with a detergent solution pH 7.0 (0.01 mM 3-(Decyldimethylammonio)propanesulfonate inner salt (SB 3–10; Sigma), 10 mM Tris, 1 mM EDTA) for 5 min at room temperature with occasional vortexing before pelleting the S^0 by centrifuging at 450 g for 30 s. The treatment was repeated four times and supernatants containing the detached cells pooled and cells collected before proteomic analysis (as above). All gels of the same condition were run in triplicate.

Protein spots were regarded as differentially expressed if they showed the following characteristics: (i) reproducibility in all three gels of the same condition; (ii) the fold change between the two conditions was ≥2.0; and (iii) the fold change between conditions was significant with a probability of 95% according to one-way ANOVA testing. Spots of interest were excised from the gel, destained, and digested with sequencing grade modified trypsin (Promega) according to standard procedures for matrix-assisted laser desorption/ionization time-of-flight (MALDI-ToF) mass spectrometry (Shevchenko et al., 1996; Pandey et al., 2000). Subsequently, tryptic digests were spotted on a MALDI target plate and co-crystallized with α-cyana-4-hydroxy-cinnamic acid solution (Agilent Technologies). Mass spectra were acquired with a Voyager DE-STR mass spectrometer (Applied Biosystems) and analyzed using DataExplorer (Applied Biosystems). External calibration with premixed standard peptides (Sequenzyme Peptide Mass Standard Kit, Applied Biosystems) was performed. Peptide mass fingerprints (PMFs) of mass spectra were searched against a local database containing the *A. caldus*^{T} draft genome sequence (NZ_ACVD00000000.1) using Mascot with the following search parameters: (i) two missed cleavages; (ii) peptide mass tolerance of 50 ppm; and (iii) variable modifications [carbamidomethyl (C), oxidation (M), propionamide (C)]. Hits in the local database with a Mowse score > 47 were significant at a confidence level of 95%. Two samples were analyzed by Edman degradation performed at the Protein Analysis Center, Karolinska Institute, Stockholm, Sweden. For more detailed functional information of identified proteins the Biocyc database[6] was queried and InterProScan signature recognition search[7] was performed.

In order to rule out any contaminating proteins originating from the biological S^0, 2D gels were run from samples prepared by suspending the S^0 in lysis buffer and sonicating. Control gels were stained with silver (Blum et al., 1987) and no protein spots were detected (data not shown).

RESULTS

BIOINFORMATIC RECONSTRUCTION OF *A. CALDUS* ISC METABOLISM

A detailed analysis of the genes present in the draft genome sequence of *A. caldus*^{T} revealed genes for ISC oxidation that are common to *A. ferrooxidans* [sulfide quinone reductase (*sqr*), *doxD*, and *tth*] (Valdes et al., 2008) and other microbial representatives from extreme acidic environments. *A. caldus* also has gene candidates potentially encoding components of the Sox sulfur oxidizing system and Sor, which are not present in its close relative *A. ferrooxidans*. The gene clusters are presented in **Figure 1A** while the bioinformatic reconstruction of *A. caldus* ISC metabolism is presented in **Figure 1B**.

The first documented step in ISC oxidation is the transition of sulfide to S^o. In Gram-negative bacteria, this reaction is carried out by the usually membrane bound Sqr. This reaction can also be catalyzed by membrane bound FCC sulfide dehydrogenase. The enzymatic activity of Sqr (EC 1.8.5.-) has been purified from *A. ferrooxidans* membranes (Wakai et al., 2007). A sulfide oxidizing activity has been identified in *A. caldus* but the enzyme has not been identified (Hallberg et al., 1996b). Furthermore, one of the three *sqr* copies present in the *A. ferrooxidans* genome is reported to be involved in ISC metabolism (Quatrini et al., 2006, 2009). In *A. caldus*, an ortholog of the *sqr* (*sqr*-1) was identified that was divergently oriented from a gene potentially encoding Sor, that participates in the utilization of S^0 as energy source in several

[6]http://biocyc.org/

[7]http://www.ebi.ac.uk/Tools/InterProScan/

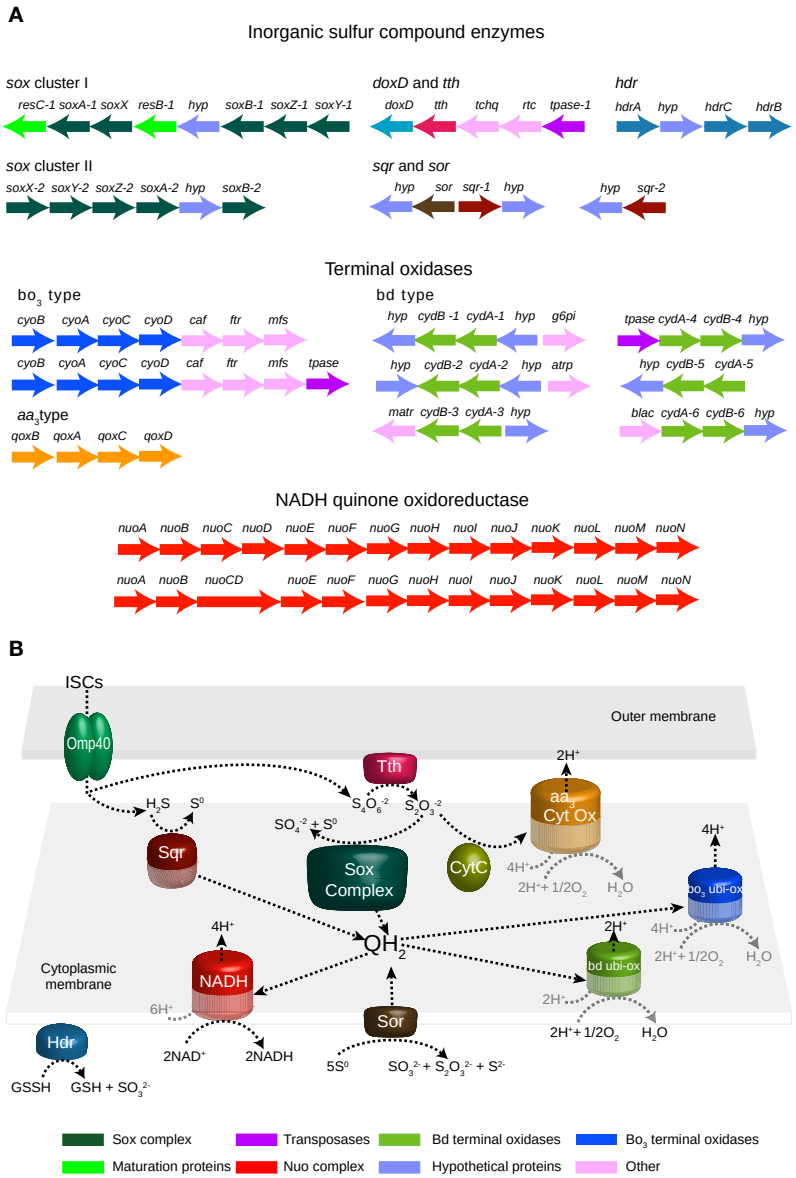

FIGURE 1 | Gene clusters of enzymes potentially involved in inorganic sulfur compound (ISC) metabolism as well as gene clusters of terminal oxidases and the NADH quinone-oxidoreductase complex as predicted by bioinformatic analysis of the *A. caldus* genome sequence (A). Suggested model for ISC metabolism in *A. caldus* (B). Abbreviations: *sox*, sulfur oxidation system; *doxD*, thiosulfate:quinol oxidoreductase; *tth*, tetrathionate hydrolase; *hdr*, heterodisulfide reductase; *sqr*, sulfide quinone reductase; *sor*, sulfur oxygenase reductase; *hyp*, hypothetical protein; *caf*, cytochrome oxidase assembly factor; *ftr*, heme O synthase, protoheme IX farnesyltranferase; *g6pi*, glucose 6-p isomerase; *mfs*, major facilitator superfamily protein; *atrp*, putative amino acid transporter; *matr*, putative malic acid transporter; *blac*, beta lactamase; *tpase*, transposase; *tchq*, two component system – histidine quinase; *rtc*, two component system – response regulator.

organisms (Urich et al., 2004). The product of the *A. caldus sqr*-1 shares 40% similarity with another putative *sqr* ortholog (*sqr*-2) identified in the draft genome sequence. This latter copy has a similar gene context to *sqr-3* from *A. ferrooxidans* and shares a 62% similarity to this protein. Although Sqr representatives belong to a large and considerably variable gene family of the pyridine nucleotide-disulfide oxido-reductases (Pfam: PF07992), the high similarity plus the conservation of gene context observed with *A. ferrooxidans* strongly suggests similar functional properties.

Another enzyme reported to be involved in ISC metabolism is Tth. The activity of this enzyme has been detected in several acidithiobacilli (Hallberg et al., 1996b; Brasseur et al., 2004). An inspection of the draft genome of *A. caldus* reveals the presence of a candidate *tth* upstream of *doxD* (**Figure 1A**). The putative Tth of *A. caldus* shares 71% similarity with the Tth of *A. ferrooxidans*, indicating their high similarity orthologous relationship. The Tth of both sequenced acidithiobacilli have a conserved pyrrolo-quinoline quinone (PQQ) domain (Pfam: PF01011). Although Tth's are

predicted to be external membrane proteins, experimental evidence showed that the *A. caldus* Tth is a soluble periplasmic protein with maximum activity at pH 3 (Bugaytsova and Lindström, 2004). Furthermore, the *tth* gene cluster has been recently studied (Rzhepishevska et al., 2007).

In contrast to the enzymes described above, the Sox sulfur oxidizing system has not been found in any microorganisms from the *Acidithiobacillus* genus. However, the bioinformatics analyses identified the presence of two gene clusters potentially encoding components of the Sox system. The *A. caldus* Sox complex is predicted to be formed by three periplasmic components (referred to as core TOMES): SoxAX, SoxYZ, and SoxB (**Figure 1A**). Our bioinformatics inspection did not identify *soxCD* orthologs in the draft genome sequence of *A. caldus*; however we cannot disregard the presence of these genes until the *A. caldus* genome sequence is finished. Nevertheless, based on the model for ISC metabolism in the green sulfur bacterium *Chlorobaculum tepidum* proposed by Sakurai et al. (2010) it can be predicted that the *A. caldus* core TOMES is able to oxidize thiosulfate with the possible accumulation of S^0 globules in the periplasm and it may be able to oxidize sulfite (Friedrich et al., 2001). No candidates for the enzymes adenylylphosphosulfate (APS) reductase or sulfate adenylyltransferases, which consecutively oxidize sulfite via an indirect pathway, have been found in the genome of *A. caldus*. However, an oxidoreductase molybdopterin-binding protein (ACA_1585) was identified as a possible sulfite oxidizing enzyme catalyzing the direct oxidation of sulfite to sulfate. ACA_1585 has a molybdopterin-binding domain (PF00174) and a twin-arginine translocation pathway signal sequence. It lacks a dimerization domain and an N-terminal heme domain. Furthermore, no additional putative subunits containing heme domains have been detected. ACA_1585 has 26% similarity with the sulfite oxidizing enzyme DraSO from *Deinococcus radiodurans* which was proposed to be a novel sulfite oxidizing enzyme without a heme domain (D'Errico et al., 2006).

Another enzyme involved in *A. caldus* ISC metabolism not found in *A. ferrooxidans* is Sor (one copy of *sor* was identified). The predicted protein shows a characteristic domain of the Sor family (Pfam: PF07682) and all activity-critical residues based on structural and experimental data (Urich et al., 2006). Furthermore, the predicted cytoplasmic location of the *A. caldus* Sor enzyme agrees with experimental data obtained from *A. tengchongensis* and *Escherichia coli* transformants (Chen et al., 2005). The *sor* was found adjacent and divergently arranged from *sqr*-1 (**Figure 1A**). This suggests the presence of potentially shared regulatory regions that could be co-regulating both enzymes, catalyzing successive reactions, and thus providing an adaptive strategy. Recently, the enzyme activity of Sor has been reported to be present in *A. caldus*-like strains (Janosch et al., 2009). However, it is still unknown how its substrate (S_8) is incorporated in to the cell or how the resulting products (S^0, H_2S, and $S_2O_3^{-2}$) are excreted. Furthermore, heterodisulfide reductase (Hdr) has been postulated to be involved in *A. ferrooxidans* S^0 oxidation (Quatrini et al., 2009) and is up-regulated during aerobic growth on solid S^0 (unpublished data). In *A. caldus* two orthologs of each HdrABC subunit have been found. Both putative HdrA subunits (ACA_1473, ACA_2418) are flavoproteins with a FAD binding site and they also contain the conserved four cysteine residues ($CXGXRDX_{6-8}CSX_2CC$) for binding of a Fe–S cluster. The putative HdrB, ACA_2421, contains two typical cysteine rich regions whereas the second putative HdrB subunit, ACA_2417, contains only one such region. The remaining subunit, HdrC, is represented by ACA_2376 and ACA_2420 both containing the 4F–4S ferredoxin iron–sulfur binding domain. ACA_2418, ACA_2421, and ACA_2420 are embedded in the gene cluster *hdrA hyp hdrC hdrB* (**Figure 1A**). All putative *A. caldus* Hdr subunits showed >90% similarity to the respective *A. ferrooxidans* Hdr subunits. As previously shown for *A. ferrooxidans* (Quatrini et al., 2009), the similarity to Hdr of other acidophilic sulfur oxidizers is significant whereas the similarity of the *A. caldus* putative HdrABC to their respective subunits of the methanogenic archaea *Methanothermobacter marburgensis* is only around 30%.

It has been shown that sulfur oxidizing bacteria which lack $Sox(CD)_2$ utilize the reverse dissimilatory sulfite reductase (DsrAB) for the oxidation of S^0 to sulfite (reviewed in Friedrich et al., 2001; Ghosh and Dam, 2009, and Sakurai et al., 2010). In *Allochromatium vinsum*, DsrAB is encoded with 13 other Dsr proteins in a cluster (Dahl et al., 2005) also containing DsrEFH and DsrC. The latter are proposed to be involved in S^0 substrate binding and transport of S^0 from the periplasmic S^0 globules to the cytoplasm (Cort et al., 2008). *Escherichia coli* DsrEFH and DsrC homologs (TusBCD and TusE) interact in a S^0 relay system during 2-thiouridine biosynthesis (Ikeuchi et al., 2006). Although no homologs of *dsr* were found in the *A. caldus* draft genome sequence, several potential DsrE-like proteins containing the characteristic DsrE/DsrF-like family features (Pfam 02635) were detected. All of those were annotated as hypothetical proteins (ACA_0867, ACA_0091, ACA_2522, ACA_0556, ACA_1583, ACA_1441, and ACA_2423) and putatively play a role in S^0 binding and transport. Additionally, several candidates for the transport of extracellular S^0 to the cytoplasm have been proposed for green sulfur bacteria (Frigaard and Bryant, 2008a,b; Sakurai et al., 2010). One possibility is that the thioredoxin SoxW acts together with thiol:disulfide interchange protein DsbD within the periplasm in transferring S^0 across the inner membrane (Sakurai et al., 2010). One candidate gene was predicted that potentially encodes a DsbC ortholog (ACA_2033) with similar functions as DsbD. DsbC thiol:disulfide interchange protein ACA_2033 exhibits a conserved N-terminal domain of the disulfide bond isomerase DsbC family (Pfam10411). It has been reported that members of this protein family are responsible for the formation of disulfide bonds and function as a disulfide bond isomerase during oxidative protein-folding in the bacterial periplasm (Hiniker et al., 2005). No homolog of SoxW has been found in *A. caldus*; however, other thioredoxins might fulfill the same function.

A. caldus is also predicted to contain two gene clusters potentially encoding components of the NADH quinone-oxidoreductase complex (EC 1.6.5.3) as has been observed in *Azotobacter vinelandii* (Bertsova et al., 2001). In addition, six *cydAB* copies possibly encoding subunits of Qox-*bd* (EC 1.10.3.-) terminal oxidase and one gene cluster that might code for a putative *aa_3-type* terminal oxidase were detected. The analysis also revealed the presence of two copies of the cytochrome *o* (*cyoBACD-caf-ftr-mfs*) gene cluster (Cyo-1 and Cyo-2), sharing 89 and 75% similarity with orthologs in *A. ferrooxidans*. This gene redundancy could have several explanations including: (i) to provide regulatory and pathway flexibility to confront environmental changes such as oxygen availability

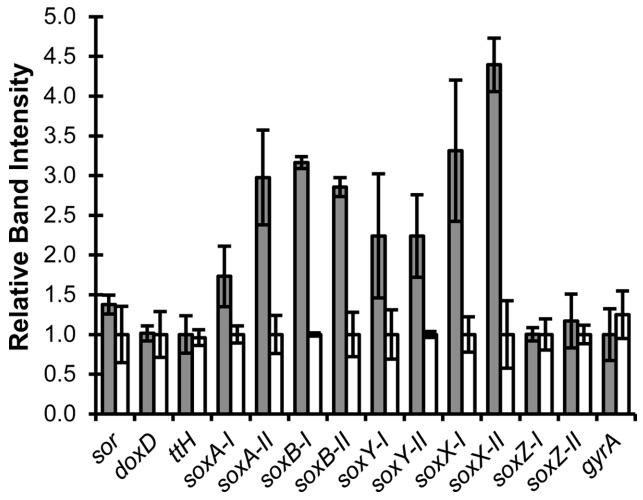

FIGURE 2 | RNA transcript profiles of selected genes predicted to be involved in *A. caldus* inorganic sulfur compound metabolism. Shown are the means of relative band intensities from semi quantitative RT-PCR products of three to four replicates with standard deviations. RNA was extracted from cells grown on tetrathionate (gray columns) or S^0 (white columns).

(*bo* and *bd* complexes have different O_2 affinities); or (ii) to manage ISC oxidizing complexes that introduce electrons at variable places in the electron transport chain (e.g., quinol-level for SQR and cytochrome *c*-level for Sox).

RNA TRANSCRIPT PROFILES OF SELECTED ISC GENES

Reverse transcription-PCR showed that all assayed genes were transcribed during growth on tetrathionate and S^0 (**Figure 2**). No significant changes in transcript levels were detected for *sor*, *doxD*, *tth*, *soxZ*-I, and *soxZ*-II. The remaining *sox* cluster genes were significantly up-regulated during growth on tetrathionate. The similar RNA levels for *soxZ*-I and *soxZ*-II during growth on tetrathionate and S^0 was unexpected as both genes would be expected to be co-transcribed with their respective gene clusters. With the exception of the *soxA* transcript, the transcript levels of both *sox* clusters followed the same trends indicating that both were involved in ISC metabolism. The control gene, *gyrA*, displayed similar transcription levels under both conditions.

PROTEIN EXPRESSION DURING GROWTH ON S^0 VERSUS TETRATHIONATE

Proteomic analysis yielded 115 identifications of differentially expressed protein spots (**Figures 3 and 4**; **Table A1** in Appendix). Forty-three proteins were up-regulated on tetrathionate (12 in soluble and 31 in membrane fraction) and 30 uniquely found on tetrathionate gels (21 in soluble and 9 in membrane fraction). During growth on S^0, 23 protein spots were up-regulated (15 in soluble and 8 in membrane fraction) and 19 were unique (11 in soluble and 8 in membrane fraction). Several protein spots yielded the same identification which indicated protein fragmentation, post translational modification, or the protein was up-regulated in both the soluble and membrane enriched fractions. Protein designations are given in parenthesis with their match ID as designated by Melanie including a capital letter S specifying soluble fraction and M for membrane enriched fractions.

No putative proteins belonging to NADH quinine-oxidoreductase or terminal oxidases were found differentially expressed in the various conditions tested. However, based on the bioinformatic reconstruction the involvement of NADH quinone-oxidoreductase complex and terminal oxidases in the *A. caldus* ISC metabolism was suggested. Therefore, these complexes were represented in the proposed model (**Figure 1B**).

Proteins involved in ISC metabolism

Proteins encoded within the two Sox clusters were up-regulated in gels from tetrathionate grown bacteria including SoxB-I (M793) and hypothetical protein ACA_2320 (S524) encoded in *sox* cluster I; as well as SoxA-II (S356, S538, S539), SoxZ-II (S10), and hypothetical protein ACA_2393 (S34) from *sox* cluster II. These findings clearly suggest an involvement of proteins encoded by both Sox clusters in ISC metabolism during growth on tetrathionate. Furthermore, both Sqr-1 (S260) and Sqr-2 (M300) were identified as up-regulated on tetrathionate. A DsrE/F-like hypothetical protein ACA_0867 (S17, S518, M13), potentially involved in S^0 binding and transport, was up-regulated on tetrathionate and subunit C of CoB–CoM heterodisulfide reductase (S543, S544; ACA_2420) was a unique protein spot on tetrathionate gels. In contrast, HdrA (S462; ACA_2418) was found as a unique protein spot in S^0 gels while the DsrE/F-like hypothetical protein ACA_1583 (S9) and DsbC thiol:disulfide interchange protein ACA_2033 (S358) were up-regulated on S^0.

General trends in the proteome of tetrathionate grown A. caldus

Several proteins relevant in signal transduction were up-regulated in tetrathionate grown cells, i.e., chemotaxis protein CheV (S151, M735), putative sensory histidine kinase YfhA (S577), nitrogen regulation protein NRI (M 776), and hypothetical protein ACA_1270 (M277) containing a PAS domain fold involved in signaling proteins. However, the signature feature of the tetrathionate grown proteome was up-regulation of proteins involved in central carbon metabolism, cell division, amino acid biosynthesis, fatty acid biosynthesis, translation, and DNA repair. The up-regulated central carbon metabolism proteins included aspartate aminotransferase (S571), dihydrolipoamide dehydrogenase (S594), fructose bisphosphate aldolase (M248), and phophoglucomutase (M368). A few proteins of central carbon metabolism were up-regulated in S^0 grown cells those including 6-phosphogluconate dehydrogenase (S154) and HAD-superfamily hydrolase (M71). Proteins involved in cell division were solely found up-regulated on gels of tetrathionate grown cells such as FtsA (M262), FtsZ (M227), and FtsH (M386, M388, M513). Four proteins involved in amino acid biosynthesis and degradation (S549, S694, M353, M755) and three involved in fatty acid biosynthesis (M179, M309, M726) were up-regulated in tetrathionate grown cells. No proteins of this group were up-regulated in S^0 grown cells. Another characteristic group consisted of translation related proteins which included two different translation elongation factors (S217, S388, M254, M521), four different tRNA synthetases (S572, S625, M431, M508), and one amidotransferase (S702) up-regulated on tetrathionate; whereas only one ribosomal protein (S338) was detected up-regulated in S^0 grown cells. Proteins involved in DNA repair included a MutS2 family protein identified in two protein spots (M344, M781) and DNA repair protein RecN (M362).

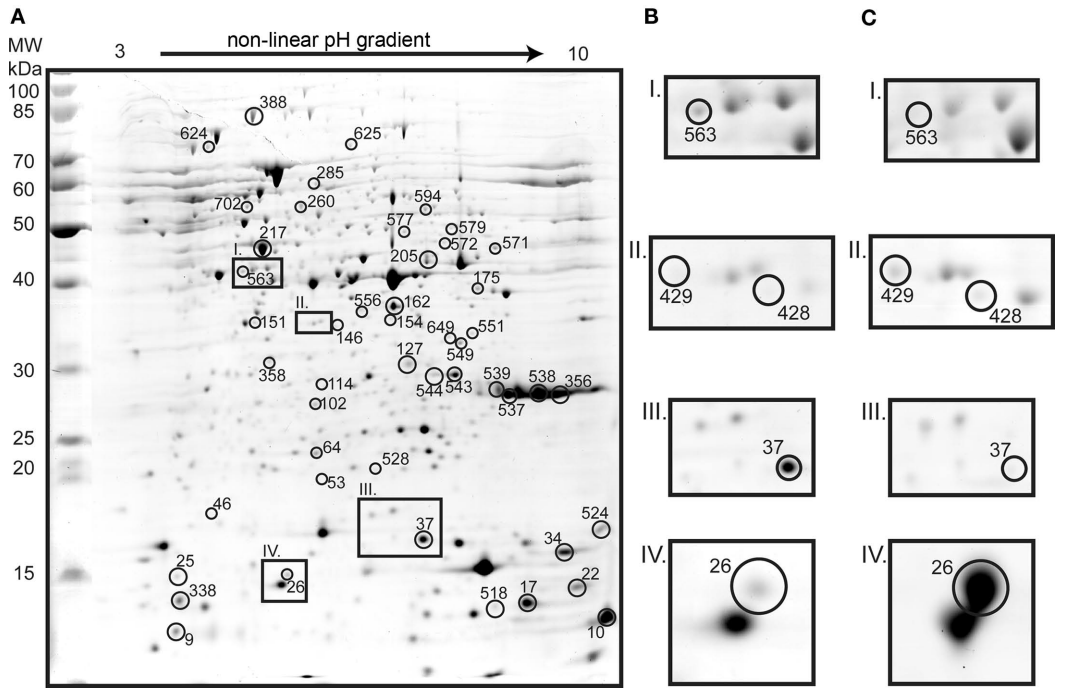

FIGURE 3 | Two dimension gel of the *A. caldus* soluble proteome from cells grown on tetrathionate (**A**; identified spots are marked with circles and the numbers indicate match IDs given without S in the figure). Inset frames show tetrathionate **(B)** and S^0 **(C)** conditions: Radical SAM domain protein (spot S563) unique in tetrathionate grown cells (I); heat shock protein GroEL (S429 and S428) unique in S^0 grown cells (II); twin-arginine translocation protein TatA (S37) which was 3.8-fold up-regulated in tetrathionate (III); and heat shock protein Hsp20 (S26) that was 8.6-fold up-regulated in S^0 grown cells (IV).

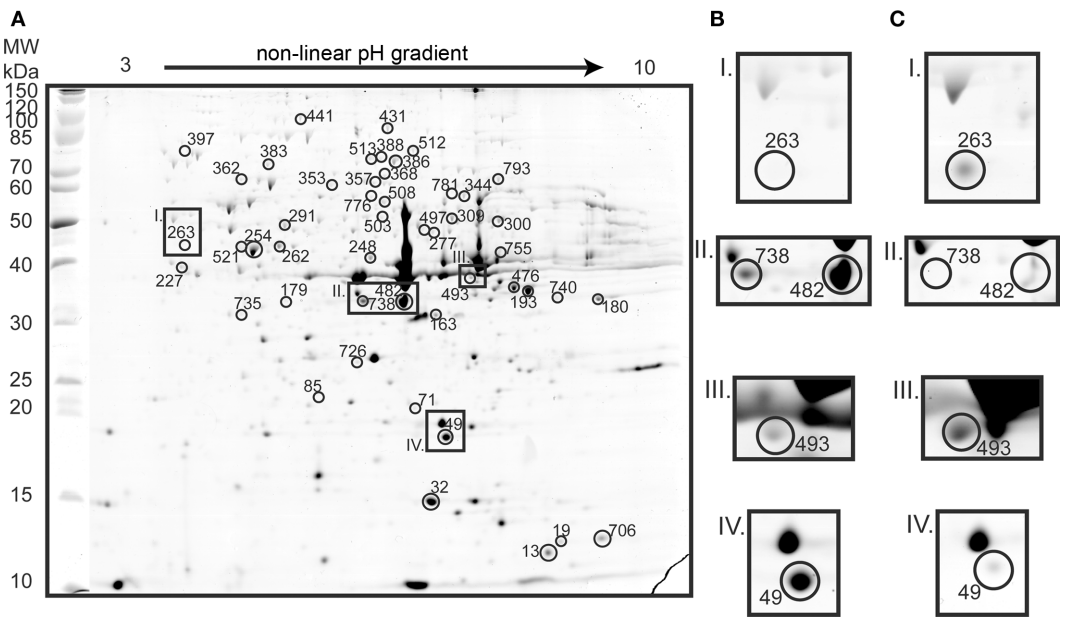

FIGURE 4 | Two dimension gel of the *A. caldus* membrane enriched proteome on tetrathionate (**A**; identified proteins indicated with circles and match IDs given without M in the figure). Inset frames are presented for tetrathionate **(B)** and for S^0 **(C)** conditions: Carboxysome shell protein CsoS1 (spot M263) that was 6.1-fold up-regulated in S^0 grown cells (I); two spots identified as hypothetical protein ACA_1144 that were unique (M738) and 10.7-fold up-regulated (M482) in gels from tetrathionate grown cells (II); type 1 secretion outer membrane protein (M493) that was 2.4-fold up-regulated in S^0 grown cells (III); and a putative lipoprotein (M49) which was 10.3-fold up-regulated on tetrathionate (IV).

Increased expression of proteins with central functions is commonly attributed to an increased growth rate. However, the samples originated from continuous cultures grown at identical dilution rates, meaning that bacteria were theoretically maintained at the same growth rate. Therefore, it was more likely that the observed trends signified down-regulation of central functions in the S^0 grown cells due to a stress response. Nevertheless, the observed results motivated the proteomic investigation of sessile and planktonic *A. caldus* grown in S^0 batch cultures as only the planktonic sub-population was investigated for the comparison of growth on tetrathionate and S^0.

General trends in the proteome of S^0 grown A. caldus

The most striking characteristic of the proteome of S^0 grown cells was the high number of up-regulated chaperones and proteases: GroEL (S114, S146, S409, S413, S416, S425, S428, S429, S435, S436), heat shock protein Hsp20 (S26, S46), DnaK (M397), ClpB (M441), and protease Do (M605). In contrast, the only chaperone up-regulated during growth on tetrathionate was HscA (S624). This indicated a stress response during growth on S^0. It should be noted that GroEL has been detected in many protein spots most of them with low molecular weight in 2D gels (**Figure 3**, **Table A1** in Appendix) indicating fragmentation of the protein. The cause of this fragmentation remains unknown. A second distinguishing feature of the S^0 grown proteome was up-regulation of proteins involved in CO_2 fixation, namely ribulose bisphosphate carboxylase large chain (M503) and carboxysome shell protein CsoS1 (M263, M530). However, the reasons for up-regulation of proteins related to CO_2 fixation remain unclear. Additionally, stringent starvation protein A (S102) and flagella basal-body rod protein FlgC (S205) were up-regulated on S^0. Stringent starvation protein A is believed to be important for stress response during stationary phase and nutrient limitation in *E. coli* (Williams et al., 1994). The up-regulation of FlgC which is part of the basal body in flagella points at an increase of flagella and the importance of cell motility in S^0 grown cells to be able to attach to the solid substrate.

Proteins up-regulated under both conditions

In one case, a two component protein was identified in both conditions whereas in other cases proteins sharing a similar function could not be clearly attributed to either condition. Those included proteins involved in protein transport such as an efflux transporter (M180, M740) and Twin-arginine translocation protein TatA (S37, M32) which were up-regulated in tetrathionate grown cells. While in S^0 grown cells protein export chaperone (S25) and Type I secretion outer membrane protein, TolC precursor (M497) were up-regulated. A two component protein was found up-regulated on tetrathionate (M291) and as a unique spot in S^0 gels (M607). The two spots were in close proximity on the gels; however the unique spot traveled with slightly larger molecular weight and more basic isoelectric point suggesting post translational modification. This protein is encoded together with the signal transduction histidine kinase up-stream of *sox* cluster II indicating that this two component system might be involved in its regulation.

PROTEIN EXPRESSION DURING PLANKTONIC VERSUS SESSILE GROWTH ON S^0

In 2D gels of planktonic *A. caldus*, three up-regulated and three unique protein spots were identified. Based on characteristic peaks in mass spectra an additional six protein spots up-regulated in planktonic cells were revealed to be the same protein. The identification of this protein could neither be determined by MALDI-ToF nor by Edman degradation. From gels of sessile cells, 22 up-regulated protein spots were identified (**Figure 5**; **Table A2** in Appendix).

Several of the proteins identified from planktonic cells were also found up-regulated in tetrathionate grown cells, i.e., TatA (64), Sqr-1 (492), and hypothetical protein ACA_0867 (826 and 827). In addition, SoxY-I (841) and hypothetical protein ACA_2219 (118) were identified. Proteins up-regulated in gels of sessile cells comprised characteristic proteins from tetrathionate grown and S^0 grown proteomes as well as proteins not identified from other gels. S^0 characteristic proteins included the chaperones GroEL and DnaK (329, 541, 543, and 556), HdrA (382; ACA_2418), and proteins involved in CO_2 fixation such as ribulose bisphosphate carboxylase large chain (258) and rubisco activation protein CbbQ (280). Tetrathionate associated proteins consisted of peptidyl-prolyl cis-trans isomerase ppiD (213), CoB–CoM HdrC (238; ACA_2420), proteins involved in amino acid biosynthesis (442, 447, 455, 515), two central carbon metabolism proteins (364, 408), and a single-stranded DNA-binding protein involved in DNA replication (70). The up-regulation of proteins involved in amino acid biosynthesis and central carbon metabolism suggests that sessile cells are less starved than planktonic cells. CoB–CoM HdrB (395; ACA_2421) was not previously detected but was found up-regulated in gels of sessile bacteria. Additionally, twitching motility protein (325) and 40-residue YVTN family β-propeller repeat protein (404) were up-regulated in gels of sessile cells. Twitching motility protein is required for twitching motility and social gliding which allows Gram-negative bacteria to move along surfaces (Merz et al., 2000). The YVTN domain is present in surface layer proteins of archaea (Jing et al., 2002) which protect cells from the environment and have been shown to be involved in cell to cell association in *Methanosarcina mazei* (Mayerhofer et al., 1998).

DISCUSSION

ISC METABOLISM IN *A. CALDUS*

A model has been constructed for ISC oxidation and electron transport based upon gene predictions and proteomics data (**Figure 1B**). Tetrathionate is hydrolyzed by a periplasmic Tth with a DoxD component (Hallberg et al., 1996b; Bugaytsova and Lindström, 2004; Rzhepishevska et al., 2007). Previously, the genes encoding Tth and DoxD were shown to be up-regulated during growth on tetrathionate as compared to growth on S^0. However, this study showed the same expression levels of *tth* and *doxD* in the semi quantitative RT-PCR. Additionally, neither protein was detected in the proteomics investigation suggesting that protein levels were also similar. A possible explanation for the discrepancy between this and the previous report (Rzhepishevska et al., 2007) is that gene transcription of *tth* and *doxD* might be different in the sub-populations of S^0 grown sessile and planktonic cells (potentially explaining the previously reported large standard deviations Rzhepishevska et al., 2007). The

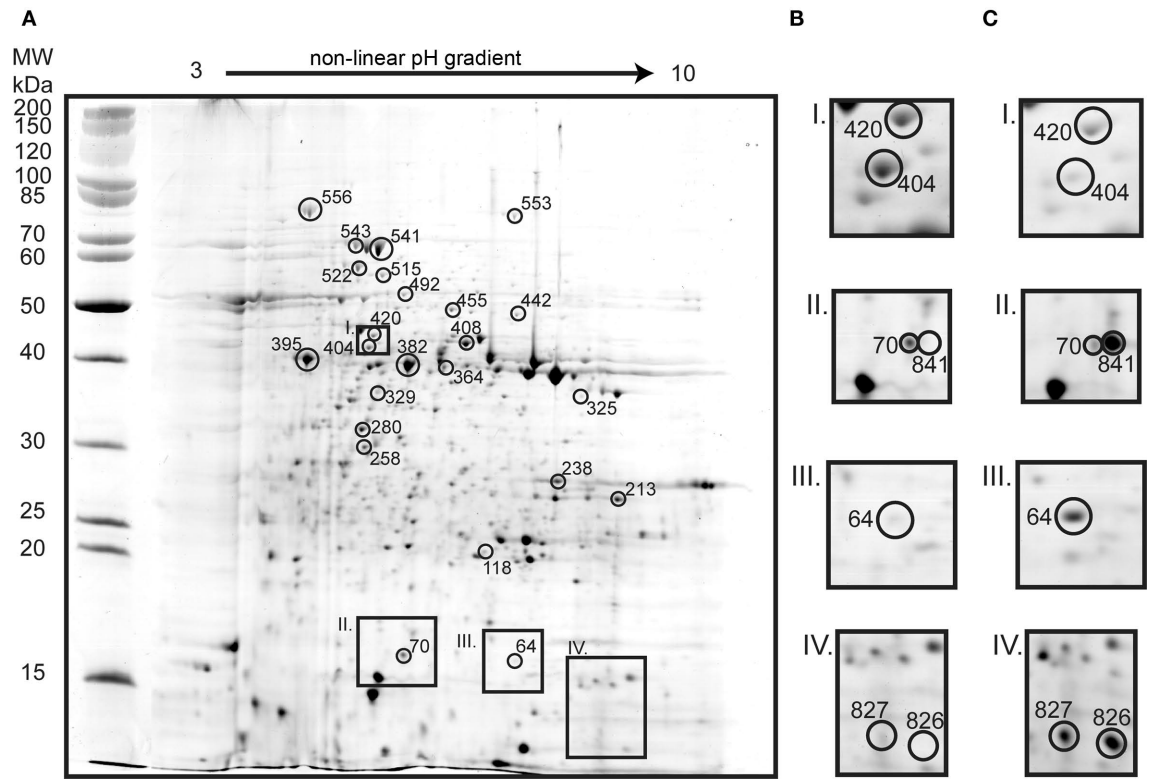

FIGURE 5 | Two dimension gel of the *A. caldus* soluble proteome of sessile cells grown on S^0 (**A**; identified proteins marked with circles and match IDs). Inset frames show sessile **(B)** and planktonic **(C)** conditions: *S*-adenosylmethionine synthetase (spot 420) and YVTN family beta-propeller repeat protein (404) that were 2.4 and spot 7.7-fold up-regulated in sessile cells (I); single-stranded DNA-binding protein (70) 3.1-fold up-regulated in sessile cells and sulfur oxidation protein SoxY (841) unique in gels from planktonic cells (II); twin-arginine translocation protein TatA (64) was up-regulated 7.9-fold in planktonic cells (III); and hypothetical protein ACA_0867 (spots 827 and 826) uniquely found in planktonic cells (IV).

role of the DoxD component is unknown as it lacks the DoxA of the thiosulfate quinine-oxidoreductase and Tth is thought to be a hydrolase (Bugaytsova and Lindström, 2004; Rzhepishevska et al., 2007). Therefore, the main product of Tth in the proposed model, thiosulfate, was suggested to be oxidized by the *A. caldus* SoxABXYZ system. The experimental data supports this view with up-regulated transcripts of both *sox* clusters as well as up-regulation of several gene products during growth on tetrathionate. As homologs of neither $Sox(CD)_2$ nor DsrAB were detected in the genome sequence of *A. caldus* to date it is proposed that the products of its core TOMES are sulfate and S^0. This aspect is further strengthened by the observation that thiosulfate oxidation has a S^0 intermediate (Hallberg et al., 1996b) and that S^0 globules have been detected in *A. caldus* when under sub-optimal conditions (Hallberg et al., 1996a). Also, sulfur globules are an obligate intermediate in *A. vinosum* thiosulfate oxidation (Pott and Dahl, 1998; Dahl et al., 2005).

The metabolism of S^0 is complicated by its hydrophobic nature which makes an activation of S^0 prior to its oxidation necessary. Potentially the DsbC (up-regulated in S^0 grown cells) was involved in transferring the S^0 equivalent from the membrane to the S^0 oxidizing enzyme as suggested for green sulfur bacteria (Sakurai et al., 2010). Additionally, it has also been suggested that sulfane sulfur is the actual substrate of the sulfur oxidizing enzyme (SDO or Hdr) in *A. ferrooxidans* (Rohwerder and Sand, 2003; Quatrini et al., 2009). The substrate for Sor is believed to be sulfur in a linear form, probably as a polysulfide. Furthermore, two hypothetical DsrE/F-like proteins were detected in the proteomics, one up-regulated on tetrathionate and the other on S^0 which might be involved in the transfer of sulfane sulfur in the course of S^0 oxidation (Dahl et al., 2005). One candidate for S^0 oxidation is Sor that catalyzes the disproportionation of S^0 to sulfite, thiosulfate, and sulfide (potentially explaining the up-regulation of Sqr in cells grown on less reduced forms of sulfur). In this study, RT-PCR data demonstrated similar levels of *sor* transcripts for growth on tetrathionate and S^0 suggesting it may be involved in ISC oxidation. A second candidate for S^0 oxidation is the trimeric complex HdrABC suggested to be involved in *A. ferrooxidans* S^0 metabolism by utilizing the proton gradient to oxidize disulfide intermediates originating from S^0 oxidation to sulfite (Quatrini et al., 2009). To date, this reverse reaction of HdrABC is purely speculative and awaits biochemical evidence. Yet, the similarities of HdrABC within acidophilic sulfur oxidizers are striking and might point to this new function of the enzyme. Additionally, *A. ferrooxidans* Hdr has been shown to be up-regulated during growth on S^0 (Quatrini et al., 2009 and unpublished data). In this study HdrA was up-regulated in S^0 grown *A. caldus*, whereas HdrC was up-regulated in tetrathionate grown cells. However, all subunits HdrABC were up-regulated in sessile compared to

planktonic cells. In our model both Sor and Hdr can oxidize S^0 and are hypothesized to comprise multiple pathways. The potential use of Hdr and/or Sor in *A. caldus* S^0 oxidation remains to be resolved. Sor or Hdr might be employed in variable growth conditions or for different (internal or external) sources of S^0. For instance, the Sor enzyme identified in *A. caldus*-like strains has an increased activity at 65°C (Janosch et al., 2009) suggesting it may be used at higher growth temperatures. The observation that DsbE-like proteins and different subunits of Hdr were up-regulated in both conditions might point to the fact that tetrathionate oxidation has a S^0 intermediate (Hallberg et al., 1996b). Following the reaction of either Sor or Hdr, the produced sulfite is oxidized to sulfate. Although no candidate for a sulfite oxidizing enzyme was detected in the proteomics a sulfite oxidase activity has been reported for *A. caldus* (Hallberg et al., 1996b) and a candidate for a sulfite oxidizing enzyme without heme domain was detected in the genome sequence. No biochemical evidence (Dopson et al., 2002) or putative gene candidates were found for involvement of the adenosine monophosphate system.

Clear trends in the protein expression of cells grown on tetrathionate versus S^0 were observed. In S^0 grown cells this included up-regulation of chaperones and a protease and down-regulation of proteins involved in central carbon metabolism, amino acid biosynthesis, fatty acid biosynthesis, cell division proteins, and DNA repair. The latter changes can be attributed to the cell's effort to conserve energy which is a feature of the general stress response.

SESSILE VERSUS PLANKTONIC *A. CALDUS*

It is believed that the stress response observed in S^0 grown sessile cells (compared to planktonic) was due to a biological phenomenon and not due to sample treatment. Several points argue in favor of this view: (i) the stress response was also apparent in S^0 grown cells when compared to tetrathionate grown cells although the treatment for both conditions was identical; and (ii) sessile cells were frozen prior to detachment which probably killed most cells conserving their proteome and making changes in the proteome of sessile cells during detachment treatment unlikely.

The *A. caldus* planktonic proteome contained up-regulated proteins similar to the expression pattern of tetrathionate grown cells; whereas, the sessile proteome contained up-regulated proteins that were described to be signature proteins of tetrathionate and S^0 grown cells. Possibly cells attached to S^0 are less starved than planktonic cells (up-regulation of proteins from central carbon metabolism) but generally more stressed than planktonic cells (up-regulation of chaperones). All three Hdr subunits were up-regulated in the sessile cells suggesting they oxidize S^0. In contrast, the planktonic sub-population may oxidize soluble ISCs (e.g., tetrathionate) potentially released from sessile cells. The growth medium of *A. caldus* grown on S^0 was tested for tetrathionate and thiosulfate. Neither compound could be detected during growth for 10 days (data not shown) potentially because the soluble ISCs were oxidized by planktonic cells before they accumulated to a detectable concentration. In addition, proteins were detected, such as a twitching motility protein involved in sessile cell motility (Merz et al., 2000) and a YVTN family beta-propeller repeat protein possibly involved in cell-to-cell interactions (Mayerhofer et al., 1998) that might also be involved in attachment to the solid substrate. Although no flagellar proteins were found up-regulated in the proteomic comparison of sessile versus planktonic cells the up-regulation of flagellar basal-body rod protein FlgC in the comparison between tetrathionate and S^0 grown cells indicated the importance of cell motility to be able to attach to the solid substrate.

Typically, planktonic and sessile sub-populations are stable (Vilain et al., 2004b) and their proteomes include many differentially expressed proteins (Vilain et al., 2004a). The proteomes and transcriptomes of biofilms have been widely studied in several neutrophilic organisms (Sauer and Camper, 2001; Oosthuizen et al., 2002; Sauer et al., 2002; Planchon et al., 2009). A transcriptomic study of biofilm and planktonic *Leptospirillum* spp. suggests acidophile biofilms are, similarly to neutrophilic biofilms, dynamic structures with distinct metabolic differences between planktonic and biofilm cells (Moreno-Paz et al., 2010). The reported differences in the proteomes between sessile and planktonic *A. caldus* sub-populations comprised a comparatively small number of differentially expressed proteins. In this case study, it may be possible that planktonic and sessile sub-populations interchanged (possibly due to vigorous stirring and shear forces exerted by the solid S^0 particles) that resulted in relatively similar proteomes.

ACKNOWLEDGMENTS

Mark Dopson wishes to thank the Swedish Research Council for financial support (Vetenskapsrådet contract number 621-2007-3537). David S. Holmes acknowledges Fondecyt 1050063, DI-UNAB 34-06, DI-UNAB 15-06/I, and a Microsoft Sponsored Research Award.

REFERENCES

Altschul, S. F., Madden, T. L., Schaffer, A. A., Zhang, J., Zhang, Z., Miller, W., and Lipman, D. J. (1997). Gapped BLAST and PSI-BLAST: a new generation of protein database search programs. *Nucleic Acids Res.* 25, 3389–3402.

Anderson, N. L. (1991). *Two Dimensional Gel Electrophoresis: Operation of the ISO-DALT System.* Rockville, MD: Large Scale Biology Press.

Bathe, S., and Norris, P. R. (2007). Ferrous iron- and sulfur-induced genes in *Sulfolobus metallicus*. *Appl. Environ. Microbiol.* 73, 2491–2497.

Bertsova, Y. V., Bogachev, A. V., and Skulachev, V. P. (2001). Noncoupled NADH:ubiquinone oxidoreductase of *Azotobacter vinelandii* is required for diazotrophic growth at high oxygen concentrations. *J. Bacteriol.* 183, 6869–6874.

Blum, H., Beier, H., and Gross, H. J. (1987). Improved silver staining of plant-proteins, RNA and DNA in polyacrylamide gels. *Electrophoresis* 8, 93–99.

Bodadilla Fazzini, R. A., and Parada, P. (2009). Analysis of sulfur metasecretome in mixed cultures of *Acidithiobacillus thiooxidans* and *Acidithiobacillus ferrooxidans*. *Adv. Mat. Res.* 71–73, 151–154.

Brasseur, G., Levican, G., Bonnefoy, V., Holmes, D., Jedlicki, E., and Lemesle-Meunier, D. (2004). Apparent redundancy of electron transfer pathways via bc_1 complexes and terminal oxidases in the extremophilic chemolithoautotrophic *Acidithiobacillus ferrooxidans*. *Biochim. Biophys. Acta* 1656, 114–126.

Bru, C., Courcelle, E., Carrère, S., Beausse, Y., Dalmar, S., and Kahn, D. (2005). The ProDom database of protein domain families: more emphasis on 3D. *Nucleic Acids Res.* 33, D212–D215.

Bryson, K., McGuffin, L. J., Marsden, R. L., Ward, J. J., Sodhi, J. S., and Jones, D. T. (2005). Protein structure prediction servers at University College London. *Nucleic Acids Res.* 33, W36–W38.

Bugaytsova, Z., and Lindström, E. B. (2004). Localization, purification and properties of a tetrathionate hydrolase from *Acidithiobacillus caldus*. *Eur. J. Biochem.* 271, 272–280.

Cardenas, J. P., Valdes, J., Quatrini, R., Duarte, F., and Holmes, D. S.

(2010). Lessons from the genomes of extremely acidophilic bacteria and archaea with special emphasis on bioleaching microorganisms. *Appl. Microbiol. Biotechnol.* 88, 605–620.

Chen, Z. W., Jiang, C. Y., She, Q., Liu, S. J., and Zhou, P. J. (2005). Key role of cysteine residues in catalysis and subcellular localization of sulfur oxygenase-reductase of *Acidianus tengchongensis*. *Appl. Environ. Microbiol.* 71, 621–628.

Cort, J. R., Selan, U., Schulte, A., Grimm, F., Kennedy, M. A., and Dahl, C. (2008). *Allochromatium vinosum* DsrC: solution-state NMR structure, redox properties, and interaction with DsrEFH, a protein essential for purple sulfur bacterial sulfur oxidation. *J. Mol. Biol.* 382, 692–707.

D'Errico, G., Di Salle, A., La Cara, F., Rossi, M., and Cannio, R. (2006). Identification and characterization of a novel bacterial sulfite oxidase with no heme binding domain from *Deinococcus radiodurans*. *J. Bacteriol.* 188, 694–701.

Dahl, C., Engels, S., Pott-Sperling, A. S., Schulte, A., Sander, J., Lubbe, Y., Deuster, O., and Brune, D. C. (2005). Novel genes of the Dsr gene cluster and evidence for close interaction of Dsr proteins during sulfur oxidation in the phototrophic sulfur bacterium *Allochromatium vinosum*. *J. Bacteriol.* 187, 1392–1404.

de Jong, G. A. H., Hazeu, W., Bos, P., and Kuenen, J. G. (1997). Polythionate degradation by tetrathionate hydrolase of *Thiobacillus ferrooxidans*. *Microbiology* 143, 499–504.

Dopson, M., and Lindström, E. B. (1999). Potential role of *Thiobacillus caldus* in arsenopyrite bioleaching. *Appl. Environ. Microbiol.* 65, 36–40.

Dopson, M., and Lindström, E. B. (2004). Analysis of community composition during moderately thermophilic bioleaching of pyrite, arsenical pyrite and chalcopyrite. *Microb. Ecol.* 48, 19–28.

Dopson, M., Lindstrom, E. B., and Hallberg, K. B. (2002). ATP generation during reduced inorganic sulfur compound oxidation by *Acidithiobacillus caldus* is exclusively due to electron transport phosphorylation. *Extremophiles* 6, 123–129.

Finn, R. D., Tate, J., Mistry, J., Coggill, P. C., Sammut, S. J., Hotz, H.-R., Ceric, G., Forslund, K., Eddy, S. R., Sonnhammer, E. L. L., and Bateman, A. (2008). The Pfam protein families database. *Nucleic Acids Res.* 36, D281–D288.

Friedrich, C. G., Bardischewsky, F., Rother, D., Quentmeier, A., and Fischer, J. (2005). Prokaryotic sulfur oxidation. *Curr. Opin. Microbiol.* 8, 253–259.

Friedrich, C. G., Rother, D., Bardischewsky, F., Quentmeier, A., and Fischer, J. (2001). Oxidation of reduced inorganic sulfur compounds by bacteria: emergence of a common mechanism? *Appl. Environ. Microbiol.* 67, 2873–2882.

Frigaard, N. U., and Bryant, D. A. (2008a). "Genomic and evolutionary perspectives on sulfur metabolism in green sulfur bacteria," in *Microbial Sulfur Metabolism*, eds C. Dahl and C. G. Friedrich (Berlin: Springer), 60–76.

Frigaard, N. U., and Bryant, D. A. (2008b). "Genomic insights into the sulfur metabolism of phototrophic green sulfur bacteria," in *Sulfur Metabolism in Phototrophic Organisms*, eds R. Hell, C. Dahl, D. B. Knaff, and T. Leustek (Berlin: Springer), 337–355.

Gehrke, T., Telegdi, J., Thierry, D., and Sand, W. (1998). Importance of extracellular polymeric substances from *Thiobacillus ferrooxidans* for bioleaching. *Appl. Environ. Microbiol.* 64, 2743–2747.

Ghosh, W., and Dam, B. (2009). Biochemistry and molecular biology of lithotrophic sulfur oxidation by taxonomically and ecologically diverse bacteria and archaea. *FEMS Microbiol. Ecol.* 33, 999–1043.

Hallberg, K. B., Dopson, M., and Lindstrom, E. B. (1996a). Arsenic toxicity is not due to a direct effect on the oxidation of reduced inorganic sulfur compounds by *Thiobacillus caldus*. *FEMS Microbiol. Lett.* 145, 409–414.

Hallberg, K. B., Dopson, M., and Lindstrom, E. B. (1996b). Reduced sulfur compound oxidation by *Thiobacillus caldus*. *J. Bacteriol.* 178, 6–11.

Hedderich, R., Hamann, N., and Bennati, M. (2005). Heterodisulfide reductase from methanogenic archaea: a new catalytic role for an iron sulfur cluster. *Biol. Chem.* 386, 961–970.

Hensen, D., Sperling, D., Truper, H. G., Brune, D. C., and Dahl, C. (2006). Thiosulphate oxidation in the phototrophic sulphur bacterium *Allochromatium vinosum*. *Mol. Microbiol.* 62, 794–810.

Hiniker, A., Collet, J. F., and Bardwell, J. C. (2005). Copper stress causes an in vivo requirement for the *Escherichia coli* disulfide isomerase DsbC. *J. Biol. Chem.* 280, 33785–33791.

Hulo, N., Bairoch, A., Bulliard, V., Cerutti, L., De Castro, E., Langendijk-Genevaux, P. S., Pagni, M., and Sigrist, C. J. (2006). The PROSITE database. *Nucleic Acids Res.* 34, D227–D230.

Ikeuchi, Y., Shigi, N., Kato, J., Nishimura, A., and Suzuki, T. (2006). Mechanistic insights into sulfur relay by multiple sulfur mediators involved in thiouridine biosynthesis at tRNA wobble positions. *Mol. Cell* 21, 97–108.

Janosch, C., Thyssen, C., Vera, M., Bonnefoy, V., Rohwerder, T., and Sand, W. (2009). Sulfur oxygenase reductase in different *Acidithiobacillus caldus*-like strains. *Adv. Mat. Res.* 71–73, 239–242.

Jing, H., Takagi, J., Liu, J. H., Lindgren, S., Zhang, R. G., Joachimiak, A., Wang, J. H., and Springer, T. A. (2002). Archaeal surface layer proteins contain beta propeller, PKD, and beta helix domains and are related to metazoan cell surface proteins. *Structure* 10, 1453–1464.

Johnson, D. B., and Hallberg, K. B. (2009). Carbon, iron and sulfur metabolism in acidophilic micro-organisms. *Adv. Microb. Physiol.* 54, 201–255.

Larkin, M. A., Blackshields, G., Brown, N. P., Chenna, R., McGettigan, P. A., McWilliam, H., Valentin, F., Wallace, I. M., Wilm, A., Lopez, R., Thompson, J. D., Gibson, T. J., and Higgins, D. G. (2007). Clustal W and Clustal X version 2.0. *Bioinformatics* 23, 2947–2948.

Mayerhofer, L. E., Conway de Macario, E., Yao, R., and Macario, A. J. (1998). Structure, organization, and expression of genes coding for envelope components in the archaeon *Methanosarcina mazei* S-6. *Arch. Microbiol.* 169, 339–345.

Merz, A. J., So, M., and Sheetz, M. P. (2000). Pilus retraction powers bacterial twitching motility. *Nature* 407, 98–102.

Molloy, M. D. (2008). Isolation of bacterial cell membrane proteins using carbonate extraction. *Methods Mol. Biol.* 424, 397–401.

Molloy, M. P., Herbert, B. R., Slade, M. B., Rabilloud, T., Nouwens, A. S., Williams, K. L., and Gooley, A. A. (2000). Proteomic analysis of the *Escherichia coli* outer membrane. *Eur. J. Biochem.* 267, 2871–2881.

Molloy, M. P., Phadke, N. D., Maddock, J. R., and Andrews, P. C. (2001). Two-dimensional electrophoresis and peptide mass fingerprinting of bacterial outer membrane proteins. *Electrophoresis* 22, 1686–1696.

Moreno-Paz, M., Gomez, M. J., Arcas, A., and Parro, V. (2010). Environmental transcriptome analysis reveals physiological differences between biofilm and planktonic modes of life of the iron oxidizing bacteria *Leptospirillum* spp. in their natural microbial community. *BMC Genomics* 11, 404. doi: 10.1186/1471-2164-11-404

Okibe, N., Gericke, M., Hallberg, K. B., and Johnson, D. B. (2003). Enumeration and characterization of acidophilic microorganisms isolated from a pilot plant stirred-tank bioleaching operation. *Appl. Environ. Microbiol.* 69, 1936–1943.

Oosthuizen, M. C., Steyn, B., Theron, J., Cosette, P., Lindsay, D., von Holy, A., and Brozel, V. S. (2002). Proteomic analysis reveals differential protein expression by *Bacillus cereus* during biofilm formation. *Appl. Environ. Microbiol.* 68, 2770–2780.

Pandey, A., Andersen, J. S., and Mann, M. (2000). Use of mass spectrometry to study signaling pathways. *Sci. STKE* 37, pl1.

Phadke, N. D., Molloy, M. P., Steinhoff, S. A., Ulintz, P. J., Andrews, P. C., and Maddock, J. R. (2001). Analysis of the outer membrane proteome of *Caulobacter crescentus* by two-dimensional electrophoresis and mass spectrometry. *Proteomics* 1, 705–720.

Planchon, S., Desvaux, M., Chafsey, I., Chambon, C., Leroy, S., Hebraud, M., and Talon, R. (2009). Comparative subproteome analysis of planktonic and sessile *Staphylococcus xylosus* C2a: new insight in cell physiology of a coagulase-negative *Staphylococcus* in biofilm. *J. Proteome Res.* 8, 1797–1809.

Pott, A. S., and Dahl, C. (1998). Sirohaem sulfite reductase and other proteins encoded by genes at the Dsr locus of *Chromatium vinosum* are involved in the oxidation of intracellular sulfur. *Microbiology* 144, 1881–1894.

Quatrini, R., Appia-Ayme, C., Denis, Y., Jedlicki, E., Holmes, D., and Bonnefoy, V. (2009). Extending the models for iron and sulfur oxidation in the extreme acidophile *Acidithiobacillus ferrooxidans*. *BMC Genomics* 10, 394. doi: 10.1186/1471-2164-10-394

Quatrini, R., Appia-Ayme, C., Denis, Y., Ratouchniak, J., Veloso, F., Valdes, J., Lefimil, C., Silver, S., Roberto, F., Orellana, O., Denizot, F., Jedlicki, E., Holmes, D., and Bonnefoy, V. (2006). Insights into the iron and sulfur energetic metabolism of *Acidithiobacillus ferrooxidans* by microarray transcriptome profiling. *Hydrometallurgy* 83, 263–272.

Ramirez, P., Guiliani, N., Valenzuela, L., Beard, S., and Jerez, C. A. (2004). Differential protein expression during growth of *Acidithiobacillus ferrooxidans* on ferrous iron, sulfur compounds, or metal sulfides. *Appl. Environ. Microbiol.* 70, 4491–4498.

Rawlings, D. E., and Johnson, D. B. (2007). The Microbiology of biomining: development and optimization of mineral-oxidizing microbial consortia. *Microbiology* 153, 315–324.

Rohwerder, T., and Sand, W. (2003). The sulfane sulfur of persulfides is the actual substrate of the sulfur-oxidizing enzymes from *Acidithiobacillus* and

Acidiphilium spp. *Microbiology* 149, 1699–1709.

Rohwerder, T., and Sand, W. (2007). Oxidation of inorganic sulfur compounds in acidophilic prokaryotes. *Engineering in Life Sciences* 7, 301-309.

Rzhepishevska, O. I., Valdés, J., Marcinkeviciene, L., Algora Gallardo, C., Meskys, R., Bonnefoy, V., Holmes, D. S., and Dopson, M. (2007). Regulation of a novel *Acidithiobacillus caldus* gene cluster involved in reduced inorganic sulfur compound metabolism. *Appl. Environ. Microbiol.* 73, 7367–7372.

Sakurai, H., Ogawa, T., Shiga, M., and Inoue, K. (2010). Inorganic sulfur oxidizing system in green sulfur bacteria. *Photosyn. Res.* 104, 163–176.

Sauer, K., and Camper, A. K. (2001). Characterization of phenotypic changes in *Pseudomonas putida* in response to surface-associated growth. *J. Bacteriol.* 183, 6579–6589.

Sauer, K., Camper, A. K., Ehrlich, G. D., Costerton, J. W., and Davies, D. G. (2002). *Pseudomonas aeruginosa* displays multiple phenotypes during development as a biofilm. *J. Bacteriol.* 184, 1140–1154.

Schippers, A., and Sand, W. (1999). Bacterial leaching of metal sulfides proceeds by two indirect mechanisms via thiosulfate or via polysulfides and sulfur. *Appl. Environ. Microbiol.* 65, 319–321.

Shevchenko, A., Wilm, M., Vorm, O., and Mann, M. (1996). Mass spectrometric sequencing of proteins silver-stained polyacrylamide gels. *Anal. Chem.* 68, 850–858.

Suzuki, I. (1999). Oxidation of inorganic sulfur compounds: chemical and enzymatic reactions. *Can. J. Microbiol.* 45, 97–105.

Takle, G. W., Toth, I. K., and Brurberg, M. B. (2007). Evaluation of reference genes for real-time RT-PCR expression studies in the plant pathogen *Pectobacterium atrosepticum*. *BMC Plant Biol.* 7, 50. doi: 10.1186/1471-2229-7-50

Tatusov, R. L., Fedorova, N. D., Jackson, J. D., Jacobs, A. R., Kiryutin, B., Koonin, E. V., Krylov, D. M., Mazumder, R., Mekhedov, S. L., Nikolskaya, A. N., Rao, B. S., Smirnov, S., Sverdlov, A. V., Vasudevan, S., Wolf, Y. I., Yin, J. J., and Natale, D. A. (2003). The COG database: an updated version includes eukaryotes. *BMC Bioinformatics* 4, 41. doi: 10.1186/1471-2105-4-41

Urich, T., Bandeiras, T. M., Leal, S. S., Rachel, R., Albrecht, T., Zimmermann, P., Scholz, C., Teixeira, M., Gomes, C. M., and Kletzin, A. (2004). The sulphur oxygenase reductase from *Acidianus ambivalens* is a multimeric protein containing a low-potential mononuclear non-haem iron centre. *Biochem. J.* 381, 137–146.

Urich, T., Gomes, C. M., Kletzin, A., and Frazao, C. (2006). X-ray Structure of a self-compartmentalizing sulfur cycle metalloenzyme. *Science* 311, 996–1000.

Wakai, S., Tsujita, M., Kikumoto, M., Manchur, M. A., Kanao, T., and Kamimura, K. (2007). Purification and characterization of sulfide:quinone oxidoreductase from an acidophilic iron-oxidizing bacterium, *Acidithiobacillus ferrooxidans*. *Biosci. Biotechnol. Biochem.* 71, 2735–2742.

Valdes, J., Pedroso, I., Quatrini, R., Dodson, R. J., Tettelin, H., Blake, R., Eisen, J. A., and Holmes, D. S. (2008). *Acidithiobacillus ferrooxidans* metabolism: from genome sequence to industrial applications. *BMC Genomics* 9, 597. doi: 10.1186/1471-2164-9-597

Valdes, J., Quatrini, R., Hallberg, K., Dopson, M., Valenzuela, P. D., and Holmes, D. S. (2009). Draft genome sequence of the extremely acidophilic bacterium *Acidithiobacillus caldus* ATCC 51756 reveals metabolic versatility in the genus *Acidithiobacillus*. *J. Bacteriol.* 191, 5877–5878.

Valenzuela, L., Chi, A., Beard, S., Shabanowitz, J., Hunt, D. F., and Jerez, C. A. (2008). "Differential-expression proteomics for the study of sulfur metabolism in the chemolithoautotrophic *Acidithiobacillus ferrooxidans*," in *Microbial Sulfur Metabolism*, eds C. Dahl and C. G. Friedrich (Berlin: Springer), 77–86.

Vilain, S., Cosette, P., Hubert, M., Lange, C., Junter, G. A., and Jouenne, T. (2004a). Comparative proteomic analysis of planktonic and immobilized *Pseudomonas aeruginosa* cells: a multivariate statistical approach. *Anal. Biochem.* 329, 120–130.

Vilain, S., Cosette, P., Zimmerlin, I., Dupont, J. P., Junter, G. A., and Jouenne, T. (2004b). Biofilm proteome: homogeneity or versatility? *J. Proteome Res.* 3, 132–136.

Williams, M. D., Ouyang, T. X., and Flickinger, M. C. (1994). Starvation-induced expression of SspA and SspB: the effects of a null mutation in sspA on *Escherichia coli* protein synthesis and survival during growth and prolonged starvation. *Mol. Microbiol.* 11, 1029–1043.

Conflict of Interest Statement: The authors declare that the research was conducted in the absence of any commercial or financial relationships that could be construed as a potential conflict of interest.

Received: 02 November 2010; accepted: 25 January 2011; published online: 10 February 2011.

Citation: Mangold S, Valdés J, Holmes DS and Dopson M (2011) Sulfur metabolism in the extreme acidophile Acidithiobacillus caldus. Front. Microbio. ***2****:17. doi: 10.3389/fmicb.2011.00017*

This article was submitted to Frontiers in Microbial Physiology and Metabolism, a specialty of Frontiers in Microbiology.

APPENDIX

Table A1 | Proteins identified from 2D gels of tetrathionate and sulfur grown *Acidithiobacillus caldus*.

Match ID[a]	Accession[b]	Protein identification	Theoretical		Experimental		Mowse score[g]	Coverage[h] (%)	Fold		
			MW (kDa)[c]	pI[d]	MW (kDa)[e]	pI[f]			E-value[i]	difference[j]	ANOVA[k]
***ACIDITHIOBACILLUS CALDUS* UP-REGULATED ON TETRATHIONATE (SOLUBLE FRACTION)**											
S10	ACA_2391	Sulfur oxidation protein SoxZ	12	9.30	12	9.32	70	60	2.6e – 04	4.0	1.5e – 02
S17	ACA_0867	Hypothetical protein ACA_0867	18	9.07	13	7.76	63	34	1.4e – 03	4.2	3.5e – 03
S37	ACA_1726	Twin-arginine translocation protein TatA	8	6.40	16	6.12	78	51	4.0e – 05	3.8	8.3e – 03
S127	ACA_2632	Pyridoxine 5′-phosphate synthase	26	6.15	29	6,05	131	54	2.2e – 10	10.5	1.6e – 03
S162	ACA_1144	Hypothetical protein ACA_1144	31	5.83	36	5.95	62	32	1.7e – 03	2.1	2.1e – 02
S217	ACA_0247	Translation elongation factor Tu	43	5.37	44	5.22	114	38	1.1e – 08	2.3	1.2e – 02
S260	ACA_0303	Sulfide-quinone reductase, sqr-1	47	5.57	54	5.44	56	17	7.6e – 03	2.2	1.2e – 03
S356	ACA_2392	Sulfur oxidation protein SoxA	32	8.77	28	8.44	49	26	3.8e – 02	2.8	2.9e – 02
S388	ACA_0248	Translation elongation factor G	64	5.12	83	5.15	150	25	2.8e – 12	3.5	1.1e – 02
S22	ACA_1957	Hypothetical protein ACA_1957	12	8.64	14	8.57	76	58	6.6e – 05	6.1	2.9e – 02
S34	ACA_2393	Protein of unknown function DUF302	19	8.96	16	8.63	89	55	3.7e – 06	6.9	4.7e – 03
S151	ACA_0832	Chemotaxis protein CheV	30	5.19	34	5.17	70	27	9.8e – 05	4.9	2.4e – 02
S518	ACA_0867	Hypothetical protein ACA_0867	18	9.07	13	7.15	59	34	3.6e – 03	unique	9.4e – 03
S524	ACA_2320	Hypothetical protein ACA_2320	17	9.15	17	9.1	73	34	1.4e – 04	unique	1.8e – 02
S528	ACA_0688	Transposase, IS4	40	9.48	19	5.85	52	16	1.6e – 02	unique	2.4e – 03
S537	ACA_1235	Peptidyl-prolyl cis-trans isomerase ppiD	28	8.54	27	7.42	61	27	2.3e – 03	unique	2.7e – 4
S538	ACA_2392	Sulfur oxidation protein SoxA	32	8.77	27	8.06	74	34	1.2e – 04	unique	1.8e – 02
S539	ACA_2392	Sulfur oxidation protein SoxA	32	8.77	28	7.23	69	24	3.7e – 04	unique	3.2e – 03
S543	ACA_2420	CoB–CoM heterodisulfide reductase subunit C	27	6.2	29	6.44	69	31	3.8e – 04	unique	1.6e – 03
S544	ACA_2420	CoB–CoM heterodisulfide reductase subunit C	27	6.2	29	6.18	68	29	4.1e – 04	unique	2.3e – 4
S549	ACA_0761	2,3,4,5-tetrahydropyridine-2,6-dicarboxylate *N*-succinyltransferase	30	6.45	31	6.57	58	21	4.0e – 03	unique	1.3e – 03
S551	ACA_2027	Methylenetetrahydrofolate dehydrogenase (NADP+)/Methenyltetrahydrofolate cyclohydrolase	32	6.62	32	6.76	101	20	2.2e – 07	unique	3.9e – 02
S556	ACA_1144	Hypothetical protein ACA_1144	31	5.83	36	5.77	58	25	4.2e – 03	unique	5.0e – 5
S563	ACA_2428	Radical SAM domain protein	43	5.17	42	5.08	66	20	7.6e – 04	unique	2.6e – 5
S571	ACA_0032	Aspartate aminotransferase	44	7.1	45	7.13	79	15	3.8e – 05	unique	2.4e – 4
S572	ACA_1795	Tyrosyl-tRNA synthetase	46	6.16	46	6.34	118	28	4.5e – 09	unique	4.5e – 4
S577	ACA_1668	Putative sensory histidine kinase YfhA	50	6.06	48	6.02	85	15	8.9e – 06	unique	2.1e – 7
S579	Mixture				49	6.43	111		2.2e – 08	unique	1.3e – 03
	ACA_0441	Fe–S protein, lactate dehydrogenase SO1521-like protein	48	6.43	49	6.43	97	30	6.2e – 07		
	ACA_0113	Serine hydroxymethyltransferase	45	6.40	49	6.43	34	18	1.2e + 00		
S594	ACA_2840	Dihydrolipoamide dehydrogenase	49	6.15	53	6.14	81	20	2.5e – 05	unique	2.0e – 7
S624	ACA_1178	Chaperone protein HscA	66	4.99	69	4.83	102	34	3.6e – 08	unique	4.2e – 4
S625	ACA_1107	Prolyl-tRNA synthetase	64	5.74	70	5.70	165	34	8.9e – 14	unique	3.4e – 02

S694	ACA_0585	2-Keto-3-deoxy-d-manno-octulosonate-8-phosphate synthase	31	6.18	32	6.39	67	22	5.9e – 04	unique	3.6e – 02
S702	ACA_0705	Aspartyl-tRNA(Asn)/Glutamyl-tRNA(Gln) amidotransferase subunit B	53	5.23	55	5.11	49	9	3.7e – 02	unique	1.5e – 4
***ACIDITHIOBACILLUS CALDUS* UP-REGULATED ON SULFUR (SOLUBLE FRACTION)**											
S9	ACA_1583	Hypothetical protein ACA_1583	13	4.68	12	4.55	110	90	2.8e – 08	2.3	2.5e – 02
S25	ACA_1132	Protein export cytoplasm chaperone protein (SecB, maintains protein to be exported in unfolded state)	16	4.68	15	4.65	60	45	3.1e – 03	3.2	2.4e – 02
S26	ACA_0889	Heat shock protein Hsp20	17	5.46	15	5.35	60	31	3.0e – 03	8.6	9.9e – 4
S46	ACA_0889	Heat shock protein Hsp20	17	5.46	17	4.86	52	31	1.7e – 02	3.5	3.4e – 02
S53	ACA_1343	Peptidoglycan-associated outer membrane lipoprotein	20	6.41	18	5.53	91	43	2.2e – 06	2.9	2.9e – 02
S64	ACA_1478	Hypothetical protein ACA_1478	20	5.52	22	5.51	62	47	1.8e – 03	3.6	4.1e – 02
S102	ACA_1210	Stringent starvation protein A	24	5.51	27	5.51	54	30	1.0e – 02	2.3	1.9e – 02
S114	ACA_2307	Heat shock protein 60 family chaperone GroEL	58	5.41	29	5.56	57	15	5.5e – 03	3.4	5.0e – 02
S146	ACA_2307	Heat shock protein 60 family chaperone GroEL	58	5.41	33	5.63	141	36	2.2e – 11	2.3	1.0e – 02
S154	ACA_0563	6-phosphogluconate dehydrogenase, NAD-binding	32	5.88	33	5.94	106	56	7.1e – 08	2.3	1.8e – 03
S175	Mixture				38	6.86	123		1.4e – 09	4.5	5.4e – 02
	ACA_2530	Membrane-fusion protein	38	7.9	38	6.86	89	40	3.3e – 06		
	ACA_2096	Glyceraldehyde-3-phosphate dehydrogenase/erythrose -4-phosphate dehydrogenase	37	7.14	38	6.86	51	33	2.5e – 02		
S205	ACA_0861	Flagellar basal-body rod protein FlgC	14	7.88	43	6.15	58	63	4.3e – 03	2.5	4.1e – 02
S285	ACA_1087	IMP cyclohydrolase/Phosphoribosylaminoimidazolecarboxamide formyltransferase	57	5.6	60	5.52	103	26	1.4e – 07	3.1	6.5e – 03
S338	ACA_0241	LSU ribosomal protein L7/L12 (L23e)	13	4.64	13	4.57	144	83	1.1e – 11	2.0	1.5e – 02
S358	ACA_2033	Thiol:disulfide interchange protein DsbG precursor	30	5.68	30	5.25	75	47	8.5e – 05	2.0	5.5e – 4
S398	ACA_1343	Peptidoglycan-associated outer membrane lipoprotein	20	6.41	16	5.55	57	30	5.5e – 03	unique	8.1e – 5
S409	ACA_2307	Heat shock protein 60 family chaperone GroEL	58	5.41	27	4.97	83	23	1.5e – 05	unique	5.7e – 03
S413	ACA_2307	Heat shock protein 60 family chaperone GroEL	58	5.41	28	5.2	50	15	3.0e – 02	unique	5.5e – 03
S416	ACA_2307	Heat shock protein 60 family chaperone GroEL	58	5.41	29	5.13	75	24	9.3e – 05	unique	1.2e – 02
S418	ACA_2632	Pyridoxine 5′-phosphate synthase	26	6.15	29	6.15	126	48	7.1e – 10	unique	3.0e – 03
S425	ACA_2307	Heat shock protein 60 family chaperone GroEL	58	5.41	33	5.17	68	24	4.2e – 04	unique	1.4e – 4
S428	ACA_2307	Heat shock protein 60 family chaperone GroEL	58	5.41	33	5.56	49	21	3.2e – 02	unique	3.2e – 03
S429	ACA_2307	Heat shock protein 60 family chaperone GroEL	58	5.41	34	5.44	56	15	6.5e – 03	unique	5.8e – 03
S435	ACA_2307	Heat shock protein 60 family chaperone GroEL	58	5.41	36	5.32	85	26	8.1e – 06	unique	2.7e – 03
S436	ACA_2307	Heat shock protein 60 family chaperone GroEL	58	5.41	37	5.33	68	22	4.6e – 04	unique	3.1e – 03
S462	ACA_2418	Heterodisulfide reductase subunit A	38	6.03	52	5.50	63	26	1.4e – 03	unique	1.9e – 02
***ACIDITHIOBACILLUS CALDUS* UP-REGULATED ON TETRATHIONATE (MEMBRANE ENRICHED FRACTION)**											
M13	ACA_0867	Hypothetical protein ACA_0867	18	9.07	12	8.69	69	34	3.6e – 04	2.3	9.9e – 03
M19	ACA_1957	Hypothetical protein ACA_1957	12	8.64	13	9.00	55	44	8.5e – 03	7.4	1.2e – 03
M32	ACA_1726	Twin-arginine translocation protein TatA	8	6.40	16	6.08	74	55	1.0e – 04	3.8	2.3e – 4
M49	ACA_1466	Putative lipoprotein	22	6.49	20	6.17	68	58	4.6e – 04	10.3	1.1e – 4

(Continued)

Table A1 | Continued

Match ID[a]	Accession[b]	Protein identification	Theoretical		Experimental		Mowse score[g]	Coverage[h] (%)	Fold		
			MW (kDa)[c]	pI[d]	MW (kDa)[e]	pI[f]			E-value[i]	difference[j]	ANOVA[k]
M163	ACA_2593	Hypothetical protein ACA_2593	39	8.71	33	6.10	49	18	3.9e – 02	5.9	3.0e – 03
M179	ACA_2091	4-hydroxy-3-methylbut-2-enyl diphosphate reductase	34	5.43	36	5.43	54	21	1.1e – 02	2.1	1.8e – 02
M180	ACA_1142	Efflux transporter, RND family, MFP subunit	39	9.39	36	9.36	78	28	4.5e – 05	15.0	2.3e – 03
M193	ACA_2096	NAD-dependent glyceraldehyde-3-phosphate dehydrogenase	37	7.14	37	8.17	99	48	3.4e – 07	2.9	6.2e – 6
M227	ACA_1229	Cell division protein FtsZ	40	4.95	41	4.98	112	28	1.8e – 08	2.2	7.7e – 4
M248	ACA_2100	Fructose-bisphosphate aldolase class II	38	5.69	43	5.74	147	35	5.6e – 12	2.1	2.6e – 4
M254	ACA_0247	Translation elongation factor Tu	43	5.37	44	5.31	101	30	2.2e – 07	4.1	3.9e – 4
	ACA_1874	Translation elongation factor Tu	21	6.21	44	5.31	72	39	1.8e – 04		
M262	ACA_1228	Cell division protein FtsA	45	5.41	46	5.41	165	40	8.9e – 14	4.5	3.1e – 4
M277	ACA_1270	Hypothetical protein ACA_1270	44	6.00	50	6.08	140	36	2.8e – 11	2.3	1.5e – 02
M291	ACA_2388	Two component, sigma54 specific, transcriptional regulator, Fis family	50	5.47	51	5.43	162	33	1.8e – 13	3.0	3.0e – 4
M300	ACA_2485	Sulfide–quinone reductase, sqr-2	48	6.53	52	7.42	108	25	4.5e – 08	2.5	2.7e – 02
M309	ACA_0933	Biotin carboxylase of acetyl-CoA carboxylase	49	6.18	53	6.22	56	20	6.6e – 03	2.1	1.5e – 02
M344	ACA_2548	MutS2 family protein	55	6.24	59	6.52	48	16	4.2e – 02	2.3	1.0e – 02
M353	ACA_2547	Acetolactate synthase large subunit	63	5.69	63	5.60	52	8	1.7e – 02	2.7	1.5e – 02
M357	ACA_2234	Uptake hydrogenase large subunit	50	6.11	64	5.76	66	21	7.8e – 04	3.1	3.2e – 02
M362	ACA_1776	DNA repair protein RecN	62	5.26	66	5.27	136	33	7.1e – 11	2.5	9.2e – 03
M368	ACA_0098	Phosphoglucomutase	59	5.88	69	5.79	56	17	7.4e – 03	3.0	1.9e – 03
M383	ACA_2179	GTPase subunit of restriction endonuclease-like protein	73	5.38	74	5.37	74	18	1.2e – 04	2.8	6.1e – 03
M386	ACA_1482	Cell division protein FtsH	69	5.98	75	5.85	114	18	1.1e – 08	4.1	6.4e – 5
M388	ACA_1482	Cell division protein FtsH	69	5.98	76	5.78	80	17	2.8e – 05	9.1	9.7e – 4
M431	ACA_2689	Phenylalanyl-tRNA synthetase beta chain	88	5.89	92	5.81	151	19	2.2e – 12	2.1	4.8e – 4
M476	ACA_2096	NAD-dependent glyceraldehyde-3-phosphate dehydrogenase	37	7.14	38	7.81	93	50	1.5e – 6	2.5	1.1e – 03
M482	ACA_1144	Hypothetical protein ACA_1144	31	5.83	35	5.91	77	32	5.1e – 05	10.7	7.9e – 5
M508	ACA_0293	Cysteinyl-tRNA synthetase	53	5.83	57	5.79	80	25	2.9e – 05	2.7	2.5e – 03
M512	ACA_0317	Chemotaxis regulator - transmits chemoreceptor signals to flagelllar motor components CheY	16	6.60	80	5.96	65	36	8.3e – 04	2.4	4.7e – 02
	ACA_0548	Hypothetical protein ACA_0548	73	6.02	80	5.96	59	14	3.8e – 03		
M513	ACA_1482	Cell division protein FtsH	69	5.98	76	5.74	128	27	4.5e – 10	3.5	1.2e – 4
M521	ACA_0247	Translation elongation factor Tu	43	5.37	46	5.27	70	22	2.9e – 04	2.1	1.4e – 03
	ACA_1874	Translation elongation factor Tu	21	6.21	46	5.27	62	40	1.8e – 03		
M706	ACA_1957	Hypothetical protein ACA_1957	12	8.64	13	9.39	71	58	2.0e – 04	unique	1.4e – 02
M726	ACA_0186	Enoyl-[acyl-carrier-protein] reductase [NADH]	27	5.70	28	5.69	122	40	1.8e – 09	unique	1.5e – 02
M735	ACA_0832	Chemotaxis protein CheV	30	5.19	34	5.27	78	24	4.7e – 05	unique	3.3e – 6
M738	ACA_1144	Hypothetical protein ACA_1144	31	5.83	36	5.72	55	34	9.8e – 03	unique	2.1e – 4
M740	ACA_1142	Efflux transporter, RND family, MFP subunit	39	9.39	36	8.90	88	23	4.7e – 06	unique	8.8e – 4

M755	ACA_2748	Aminomethyltransferase	42	6.73	45	7.45	128	49	4.5e – 10	unique	7.7e – 5
M776	ACA_1984	Nitrogen regulation protein NR(I)	54	5.84	58	5.74	104	25	1.1e – 07	unique	1.8e – 4
M781	ACA_2548	MutS2 family protein	55	6.24	60	6.23	50	13	2.9e – 02	unique	9.9e – 5
M793	ACA_2317	5′-Nucleotidase domain protein	64	6.66	66	7.41	83	11	1.3e – 05	unique	8.7e – 7
***ACIDITHIOBACILLUS CALDUS* UP-REGULATED ON SULFUR (MEMBRANE ENRICHED FRACTION)**											
M71	ACA_2067	HAD-superfamily hydrolase, subfamily IA, variant 3	24	6.08	24	5.97	160	64	2.8e – 13	2.1	1.6e – 02
M85	ACA_0146	Alkyl hydroperoxide reductase subunit C-like protein	24	5.67	26	5.55	60	23	2.8e – 03	2.6	4.1e – 02
M263	ACA_2773	Carboxysome shell protein CsoS1	10	5.52	47	5.00	58	41	4.5e – 03	6.1	6.9e – 3
M397	ACA_1454	Chaperone protein DnaK	68	5.06	79	5.01	59	18	3.9e – 03	3.6	8.4e – 03
M441	ACA_2034	ClpB protein	97	5.52	100	5.49	198	25	4.5e – 17	2.7	9.0e – 4
M493	ACA_2352	Phosphate-selective porin O and P	42	5.87	39	6.70	96	29	6.9e – 07	3.3	1.6e – 02
M497	ACA_0129	Type I secretion outer membrane protein, TolC precursor	50	6.34	50	6.02	74	23	1.1e – 04	2.4	9.4e – 03
M503	ACA_2765	Ribulose bisphosphate carboxylase large chain	53	5.96	53	5.78	121	27	2.2e – 09	2.6	8.5e – 4
M530	ACA_2773	Carboxysome shell protein CsoS1	10	5.52	10	5.39	121	62	2.2e – 09	unique	1.0e – 02
	ACA_2771	Carboxysome shell protein CsoS1	10	5.58	10	5.39	78	46	4.3e – 05		
	ACA_2772	Carboxysome shell protein CsoS1	10	5.58	10	5.39	78	46	4.3e – 05		
M539	ACA_1520	Hypothetical protein ACA_1520	12	6.52	16	8.39	91	59	2.0e – 06	unique	2.8e – 4
M550	ACA_0172	1,2-dihydroxy-3-keto-5-methylthiopentene dioxygenase	21	5.10	22	5.05	77	36	5.4e – 05	unique	1.4e – 02
M553	ACA_0993	Hypothetical protein ACA_0993	25	8.98	25	8.89	141	42	2.2e – 11	unique	1.8e – 02
M565	ACA_1527	Hypothetical protein ACA_1527	32	4.74	28	4.66	57	26	6.2e – 03	unique	1.4e – 5
M605	ACA_0109	Protease Do	53	6.98	51	6.9	54	15	1.2e – 02	unique	2.1e – 02
M607	ACA_2388	Two component, sigma54 specific, transcriptional regulator, Fis family	50	5.47	52	5.33	53	16	1.4e – 02	unique	4.0e – 4
M675	ACA_2024	Outer membrane component of tripartite multidrug resistance system	51	6.14	53	5.52	75	16	9.3e – 05	unique	4.7e – 4

[a]*Match ID was generated by Melanie and refers to protein spots in* ***Figure 3*** *(soluble fraction) and* ***Figure 4*** *(membrane fraction). Match ID in Figures is given without S or M in front of numbers.*
[b]*Annotation number is that of Genebank genome annotation NZ_ACVD01000000.1.*
[c]*Predicted Molecular weight of database entry.*
[d]*Predicted isoelectric point (pI) of database entry.*
[e]*Experimental molecular weight determined by 2D-PAGE.*
[f]*Experimental pI determined by 2D-PAGE.*
[g]*Mowse score was generated by Mascot and describes the hit of a peptide mass fingerprint (PMF) search giving the probability that the hit is not a random match in the database (scores > 47 are significant with a significance threshold of 0.05).*
[h]*Sequence coverage (generated by Mascot) presents the percentage of the database hit that was covered by the submitted peptide masses of the experimentally acquired PMF.*
[i]*Expect value (generated by Mascot) is the number of hits expected by change in a database of the same size.*
[j]*Fold change was determined with Melanie. Fold changes ≥ 2.0 were regarded as differentially expressed.*
[k]*Anova test was performed for two or three replicates of each condition and spots with p-values < 0.05 were considered to be significant.*

Table A2 | Proteins identified in 2D gels from sessile and planktonic *Acidithiobacillus caldus*.

Match ID[a]	Accession[b]	Protein identification	Theoretical		Experimental		Mowse score[g]	Coverage[h] (%)	Fold		
			MW (kDa)[c]	pI[d]	MW (kDa)[e]	pI[f]			E-value[i]	difference[j]	Anova[k]
***ACIDITHIOBACILLUS CALDUS* PLANKTONIC**											
64	ACA_1726	Twin-arginine translocation protein TatA	8	6.40	16	6.33	71	51	2.1e – 04	7.9	9.0e – 03
118	ACA_2219	Hypothetical protein ACA_2219	20	6.15	20	6.11	75	31	8.9e – 05	4.2	1.4e – -03
492	ACA_0303	Sulfide–quinone reductase, sqr-1	47	5.57	52	5.56	86	35	6.5e – 06	2.4	7.2e – 5
826	ACA_0867	Hypothetical protein ACA_0867	18	9.07	14	7.18	101	61	2.2e – 07	unique	2.9e – 6
827	ACA_0867	Hypothetical protein ACA_0867	18	9.07	14	6.95	69	53	3.2e – 04	unique	5.2e – 5
841[l]	ACA_2319	Sulfur oxidation protein SoxY			16	5.65				unique	3.3e – 4
***ACIDITHIOBACILLUS CALDUS* SESSILE**											
70	ACA_1907	Single-stranded DNA-binding protein	17	5.49	16	5.59	70	66	3.0e – 04	3.1	3.1e – 02
213	ACA_1235	Peptidyl-prolyl cis-trans isomerase ppiD	28	8.54	27	7.12	56	20	6.6e – 03	2.7	1.1e – 02
238	ACA_2420	CoB–CoM heterodisulfide reductase subunit C	27	6.20	28	6.67	113	50	1.4e – 08	2.8	7.9e – 03
258	ACA_2765	Ribulose bisphosphate carboxylase large chain	53	5.96	30	5.36	68	15	4.7e – 04	2.2	5.1e – 4
280	ACA_2783	Rubisco activation protein CbbQ mod	30	5.32	32	5.32	84	35	1.2e – 05	2.4	5.3e – 5
325	ACA_2737	Twitching motility protein	39	6.50	36	6.87	102	33	1.8e – 07	2.0	1.7e – 03
329	ACA_2307	Heat shock protein 60 family chaperone GroEL	58	5.14	37	5.4	64	18	1.2e – 03	2.2	9.5e – 03
364	ACA_0002	Pyruvate dehydrogenase E1 component beta subunit	35	5.69	39	5.8	77	20	5.5e – 05	3.0	2.5e – 02
382	ACA_2418	Heterodisulfide reductase subunit A	38	6.03	40	5.57	93	34	1.5e – 06	2.4	3.6e – 4
	ACA_1473	Heterodisulfide reductase subunit A	38	5.86	40	5.57	68	28	4.3e – 04		
395	ACA_2421	CoB–CoM heterodisulfide reductase subunit B	33	5.01	41	5.03	71	56	2.3e – 04	2.1	5.9e – 4
404	ACA_0152	40-residue YVTN family beta-propeller repeat protein	96	5.98	43	5.35	49	7	3.4e – 02	7.7	4.4e – 5
408	ACA_2100	Fructose-bisphosphate aldolase class II	38	5.69	43	5.93	76	33	7.4e – 05	2.3	1.6e – 02
420	ACA_0056	*S*-adenosylmethionine synthetase	42	5.37	45	5.38	79	21	3.3e – 05	2.4	9.0e – 6
442	ACA_0500	Gamma-glutamyl phosphate reductase	46	5.87	48	6.37	109	25	3.6e – 08	2.5	1.7e – 03
447	ACA_0113	Serine hydroxymethyltransferase	45	6.4	49	6.73	71	22	2.0e – 04	5.2	8.5e – 03
455	ACA_1035	3-isopropylmalate dehydratase large subunit	51	5.69	49	5.85	107	33	5.6e – 08	2.5	1.8e – 5
515	ACA_0148	2-isopropylmalate synthase	32	5.94	56	5.43	86	29	7.3e – 06	2.5	1.7e – 03
522	ACA_0976	ATP synthase alpha chain	56	5.32	57	5.27	68	18	4.0e – 04	2.3	1.7e – 03
541	ACA_2307	Heat shock protein 60 family chaperone GroEL	58	5.14	63	5.4	96	34	7.8e – 07	3.8	7.0e – 03
543	ACA_2307	Heat shock protein 60 family chaperone GroEL	58	5.14	67	5.26	94	28	1.2e – 06	2.4	8.1e – 4
553	ACA_2095	Transketolase	73	5.95	79	6.33	77	18	5.8e – 05	3.0	5.2e – 03
556	ACA_1454	Chaperone protein DnaK	68	5.06	82	5.02	155	36	8.9e – 13	2.6	3.4e – 03

[a]*Match ID was generated by Melanie and refers to protein spots in* ***Figure 5****.*
[b]*Annotation number is that of Genebank genome annotation NZ_ACVD01000000.1.*
[c]*Predicted Molecular weight of database entry.*
[d]*Predicted isoelectric point (pI) of database entry.*
[e]*Experimental molecular weight determined by 2D-PAGE.*
[f]*Experimental pI determined by 2D-PAGE.*
[g]*Mowse score was generated by Mascot and describes the hit of a peptide mass fingerprint (PMF) search giving the probability that the hit is not a random match in the database (scores > 47 are significant with a significance threshold of 0.05).*
[h]*Sequence coverage (generated by Mascot) presents the percentage of the database hit that was covered by the submitted peptide masses of the experimentally acquired PMF.*
[i]*Expect value (generated by Mascot) is the number of hits expected by change in a database of the same size.*
[j]*Fold change was determined with Melanie. Fold changes ≥2.0 were regarded as differentially expressed.*
[k]*Anova test was performed for two or three replicates of each condition and spots with p-values < 0.05 were considered to be significant.*
[l]*Sample was analyzed by Edman degradation.*